

Advanced 
**Synthesis &
Catalysis**

Supporting Information

© Copyright Wiley-VCH Verlag GmbH & Co. KGaA, 69451 Weinheim, 2012

Supplementary Information

A New Type of Stereoselectivity in Baeyer-Villiger Reactions:

Access to *E*- and *Z*-Olefins

Zhi-Gang Zhang,^{a,b,†} Gheorghe-Doru Roiban,^{a,b,†} Juan Pablo Acevedo,^{c, †} Iakov Polyak,^a and Manfred T. Reetz^{a,b,*}

^a Max-Planck-Institut für Kohlenforschung, Kaiser-Wilhelm-Platz 1, 45470 Mülheim an der Ruhr, Germany
E-mail: reetz@mpi-muelheim.mpg.de

^b Philipps-Universität Marburg, Fachbereich Chemie, Hans-Meerwein-Strasse, 35032 Marburg, Germany

^c Facultad de Medicina y Facultad de Ingeniería y Ciencias Aplicadas, Universidad de los Andes, Santiago, Chile

† Equal contribution

Contents

Biology	4
Table S1. Choice of codon degeneracies at each site selected for saturation mutagenesis	4
Table S2. Primers used for generation of libraries A-C.....	4
Table S3. CHMO mutant Phe432Ile/Thr433Gly/Leu143Met/Phe505Cys as a catalyst in whole-cell Baeyer-Villiger reactions of ketones 3a-d with formation of lactones 4a-d	4
Chemistry	5
Preparation of 8-ethylidene-1,4-dioxaspiro[4.5]decane (S1).....	5
Preparation of 4-ethylidene-cyclohexanone (3a)	5
Preparation of 8-bromomethylene-1,4-dioxaspiro[4.5]decane (S2).....	5
Preparation of 4-(bromomethylene)cyclohexanone (3b)	6
Preparation of 4-benzylidene-cyclohexanone (3c).....	6
Preparation of ethyl 2-(4-oxocyclohexylidene)acetate (3d).....	6
Preparation of (<i>E</i>)-4-ethylidene- ϵ -caprolactone (<i>E</i> -4a).....	7
Preparation of (<i>E</i>)-4-bromomethylene- ϵ -caprolactone (<i>E</i> -4b).....	7
Preparation of (<i>Z</i>)-4-bromomethylene- ϵ -caprolactone (<i>Z</i> -4b)	8
Preparation of (<i>E</i>)-4-benzylidene- ϵ -caprolactone (<i>E</i> -4c).....	8
Preparation of ethyl (<i>Z</i>)-4-carboxymethylene- ϵ -caprolactone (<i>Z</i> -4d).....	8
Lactones behavior in reaction with nucleophiles.....	9
Preparation of (<i>E</i>)-4-(bromomethylene)-6-hydroxyhexanoic acid (S3)	9
Preparation of (<i>E</i>)-methyl 4-(bromomethylene)-6-hydroxyhexanoate (S4)	9
Preparation of (<i>E</i>)-4-benzylidene-6-hydroxyhexanoic acid (S5).....	10
Preparation of (<i>E</i>)-diethyl 3-(2-hydroxyethyl)hex-2-enedioate (<i>E</i> -5)	10
Preparation of ethyl 3-(6-oxo-3,6-dihydro-2H-pyran-4-yl)propanoate (6).....	11
QM/MM calculations	12
MM calculations.....	13
Choosing appropriate randomization sites for iterative saturation mutagenesis (ISM) and initial MM analysis	13
Analysis of the Criegee-intermediates leading to <i>E</i> - or <i>Z</i> -lactone formation	14
NMR spectra.....	17
¹ H NMR (300 MHz, CDCl ₃) and ¹³ C NMR (75 MHz, CDCl ₃) spectra of compound 3a.....	17
¹ H NMR (300 MHz, CDCl ₃) and ¹³ C NMR (75 MHz, CDCl ₃) spectra of compound 3b	18
¹ H NMR (300 MHz, CDCl ₃) and ¹³ C NMR (75 MHz, CDCl ₃) spectra of compound 3c.....	19
¹ H NMR (300 MHz, CDCl ₃) and ¹³ C NMR (75 MHz, CDCl ₃) spectra of compound 3d	20
¹ H NMR (400 MHz, CDCl ₃) and ¹³ C NMR (101 MHz, CDCl ₃) spectra of compound <i>E</i> -4a.....	21
COSY spectrum of compound <i>E</i> -4a (CDCl ₃)	22
NOESY spectrum of compound <i>E</i> -4a (CDCl ₃).....	22
¹ H NMR spectra of compounds <i>E</i> -4b and <i>Z</i> -4b (300 MHz, CDCl ₃).....	23
¹³ C NMR spectra of compounds <i>E</i> -4b and <i>Z</i> -4b (75 MHz, CDCl ₃)	23
COSY spectrum of compound <i>Z</i> -4b (CDCl ₃)	24
NOESY spectrum of compound <i>Z</i> -4b (CDCl ₃).....	24
¹ H NMR (300 MHz, CDCl ₃) and ¹³ C NMR (75 MHz, CDCl ₃) spectra of compound <i>E</i> -4c	25
¹ H NMR (300 MHz, CDCl ₃) and ¹³ C NMR (75 MHz, CDCl ₃) spectra of compound <i>Z</i> -4d.....	26
COSY spectrum of compound <i>Z</i> -4d (CDCl ₃)	27
NOESY spectrum of compound <i>Z</i> -4d (CDCl ₃).....	27
¹ H NMR (300 MHz, CDCl ₃) and ¹³ C NMR (75 MHz, CDCl ₃) spectra of compound <i>E</i> -5.....	28
¹ H NMR (300 MHz, CDCl ₃) and ¹³ C NMR (75 MHz, CDCl ₃) spectra of compound 6	29
¹ H NMR (300 MHz, CDCl ₃) and ¹³ C NMR (75 MHz, CDCl ₃) spectra of compound S2	31
¹ H NMR (300 MHz, CDCl ₃) and ¹³ C NMR (75 MHz, CDCl ₃) spectra of compound S3	32
¹ H NMR (300 MHz, CDCl ₃) and ¹³ C NMR (75 MHz, CDCl ₃) spectra of compound S4	33
¹ H NMR (300 MHz, DMSO- <i>d</i> ₆) and ¹³ C NMR (75 MHz, DMSO- <i>d</i> ₆) spectra of compound S534	33

Determination of conversion and diastereoisomeric composition (<i>cis/trans</i>)	35
GC Chromatograms	36
Preparation of (<i>E</i>)-4-ethylidene- ϵ -caprolactone (<i>E</i> -4a) resulting from biocatalytic Baeyer-Villiger reaction of 3a with WT CHMO	36
Preparation of (<i>Z</i>)-4-ethylidene- ϵ -caprolactone (<i>Z</i> -4a) resulting from biocatalytic Baeyer-Villiger reaction of 3a with Mutant CHMO	37
Preparation of (<i>E</i>)-4-bromomethylene- ϵ -caprolactone (<i>E</i> -4b) resulting from biocatalytic Baeyer-Villiger reaction of 3b with WT CHMO	38
Preparation of (<i>Z</i>)-4-bromomethylene- ϵ -caprolactone (<i>Z</i> -4b) resulting from biocatalytic Baeyer-Villiger reaction of 3b with Mutant CHMO	39
HPLC Chromatograms	40
Mixture of (<i>E</i>)-4-bromomethylene- ϵ -caprolactone (<i>E</i> -4b) and (<i>Z</i>)-4-bromomethylene- ϵ -caprolactone (<i>Z</i> -4b) (87:13 <i>trans/cis</i>)	40
Separated (<i>E</i>)-4-bromomethylene- ϵ -caprolactone (<i>E</i> -4b)	41
Separated (<i>Z</i>)-4-bromomethylene- ϵ -caprolactone (<i>Z</i> -4b)	42
X-ray data	43
Single crystal X-ray structure of compound <i>E</i> -4b	43
Figure S3 The molecular structure of <i>E</i> -4b. Atomic displacement ellipsoids are shown at the 50% probability level	43
Table S4. Atomic coordinates and equivalent isotropic displacement parameters (\AA^2)	45
Table S5. Selected bond lengths [\AA] and angles [$^\circ$].	46
Table S6. Anisotropic displacement parameters (\AA^2)	47
References	48

Table S1. Choice of codon degeneracies at each site selected for saturation mutagenesis

Library	Randomization of amino acids	Codon degeneracy	Encoded amino acids	codons	Oversampling for 95% coverage
A	Phe432	NDT	Phe, Tyr, Cys, Leu, His, Arg, Ile, Asn, Ser, Val, Asp, Gly	144	430
	Leu433	NDT	Phe, Tyr, Cys, Leu, His, Arg, Ile, Asn, Ser, Val, Asp, Gly		
B	Leu143	NNK	All twenty amino acids	32	96
C	Fhe505	NNK	All twenty amino acids	32	96

Table S2. Primers used for generation of libraries A-C

Library	Primers	Sequences
A	Forward:	5' - ACCGAATGGCCCGNDTNDTAACCTGCCGCCATCA-3'
	Reverse:	5' - TGATGGCGGCAGGTTAHNAHNCGGGCCATTCGGT-3'
B	Forward:	5' - CTGCTTTAGGCNNKTTGTCTGCGCCTAAC-3'
	Reverse:	5' - GTTAGGCGCAGACAAMNNGCCTAAAGCAG-3'
C	Forward:	5' - CACGGTTTACNNKTATCTCGGTGG-3'
	Reverse:	5' - CCACCGAGATAMNNGTAAACCGTG-3'

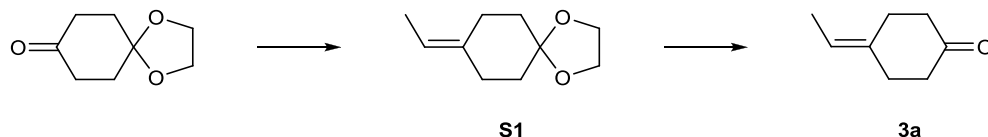
Table S3. CHMO mutant Phe432Ile/Thr433Gly/Leu143Met/Phe505Cys as a catalyst in whole-cell Baeyer-Villiger reactions of ketones 3a-d with formation of lactones 4a-d (2 mM, 100 μ mol scale, 12h).

Ketone	Product	<i>E</i> : <i>Z</i>	Conversion (%) ^[a]	Other products(%) ^[a]
3a	4a	76:24	24	16
3b	4b	20:80	30	46
3c	4c	>99:1	>99	7
3d	4d	10:90	65	37
3d	4d ^[b]	4:96	>98	9

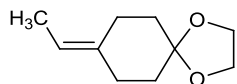
[a] By GC analysis of the crude products, the side-products being the alcohols corresponding to the ketones; [b] Experiment performed under up-scaling conditions (2 mM, 2.4 mmol scale, 12h).

Chemistry

General scheme for preparation of 4-ethylidenecyclohexanone (**3a**)

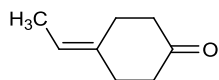


Preparation of 8-ethylidene-1,4-dioxaspiro[4.5]decane (**S1**)



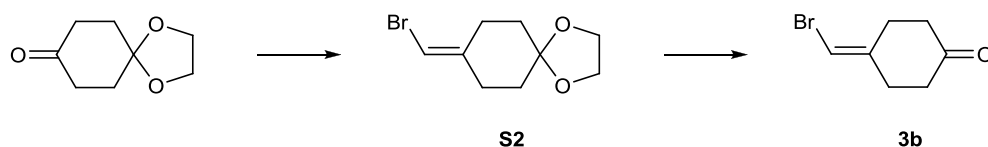
To a cooled (-70 °C) solution of ethyltriphenylphosphonium iodide (16.03 g, 38.3 mmol) in anhydrous THF (50 mL), *n*-butyllithium (15.3 mL, 2.5 M in hexane, 38.3 mmol) was added dropwise during 15 min. After 30 min stirring, 1,4-cyclohexanedione monoethylene acetal (5.44 g, 34.8 mmol) in tetrahydrofuran (50 mL) was added over 20 min and the mixture was then allowed to reach r.t. overnight. The solution was then filtered and washed with dichloromethane (3x100 mL), the combined fractions concentrated and the resulted yellow oil subjected to column chromatography to afford (**S1**) as a colorless oil (5.21 g, 89%). ($R_f=0.38$ ethyl acetate/petroleum ether=1:15); $^1\text{H NMR}$ (300 MHz, CDCl_3) $\delta=5.20$ (q, $^3J=6.7$ Hz, 1H), 3.96 (s, 4H), 2.24 (m, 4H), 1.64 (m, 4H), 1.58 (d, $^3J=6.7$ Hz, 3H); $^{13}\text{C NMR}$ (75 MHz, CDCl_3) $\delta=137.36$, 116.86, 109.28, 64.43 (2C), 36.34, 35.43, 33.62, 24.72, 13.06; MS (70 eV, EI): m/z (%): 168 [M] $^+$ (64); HRMS (EI) calcd for $\text{C}_{10}\text{H}_{16}\text{O}_2$ [M] $^+$: 168.1144; found: 168.1139.

Preparation of 4-ethylidenecyclohexanone (**3a**)

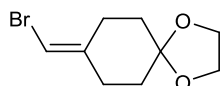


An aqueous solution of 20% H_2SO_4 (5 mL) was added over SiO_2 (20 g) in dichloromethane and then stirred for 30 min. The acetal (**S1**) dissolved in dichloromethane (30 mL) was stirred 2 hours at r.t., filtered and the organic phase washed with water. After separation and drying, the rotavaporated residue was subjected to column chromatography to afford compound **3a** as a colorless liquid (1.35 g, 78%). ($R_f=0.30$ ethyl acetate/petroleum ether=1:15); $^1\text{H NMR}$ (300 MHz, CDCl_3) $\delta=5.39$ (q, $^3J=6.8$ Hz, 1H), 2.42 (m, 8H), 1.62 (d, $^3J=6.8$ Hz, 3H); $^{13}\text{C NMR}$ (75 MHz, CDCl_3) $\delta=212.01$, 134.63, 119.48, 41.87, 40.79, 34.22, 25.86, 13.24; MS (70 eV, EI): m/z (%): 124 [M] $^+$ (80); HRMS (APCI+) calcd for $\text{C}_8\text{H}_{13}\text{O}$ [$M+H$] $^+$: 125.0961; found: 125.0960.

General scheme for preparation of 4-bromomethylidenecyclohexanone

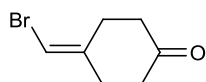


Preparation of 8-bromomethylene-1,4-dioxaspiro[4.5]decane (**S2**)¹



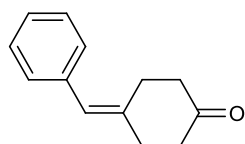
To a cooled (-70 °C) solution of bromomethyltriphenylphosphonium bromide (7.41 g, 16.9 mmol) in anhydrous tetrahydrofuran (40 mL), sodium hexamethyldisilazide (16.9 mL, 1N in tetrahydrofuran, 16.9 mmol) was added dropwise. After stirring for 1 h, 1,4-cyclohexanedione monoethylene acetal (2.21 g, 14.15 mmol) in tetrahydrofuran (10 mL) was added over 5 min and the mixture was allowed to warm at r.t. overnight. Petroleum ether (100 mL) was then added, and the resulting suspension was filtered through a short plug of celite. The filtrate was concentrated and the resulted yellow oil was subjected to column chromatography to afford compound **S2** as colorless oil (2.65 g, 80%). ($R_f=0.44$ ethyl acetate/petroleum ether=1:9); $^1\text{H NMR}$ (300 MHz, CDCl_3) $\delta=5.90$ (t, $^4J=1.2$ Hz, 1H), 3.96 (s, 4H), 2.48 (m, 2H), 2.33 (m, 2H), 1.69 (m, 4H); $^{13}\text{C NMR}$ (75 MHz, CDCl_3) $\delta=142.66, 108.42, 99.07, 64.55$ (2C), 35.52, 34.51, 32.16, 27.97; MS (70 eV, EI): m/z (%): 232 [M] $^+$ (20); HRMS (APCI+) calcd for $\text{C}_9\text{H}_{14}\text{BrO}_2$ [$M+H$] $^+$: 233.0172, 235.0152; found: 233.0170, 235.0149.

Preparation of 4-(bromomethylene)cyclohexanone (**3b**)



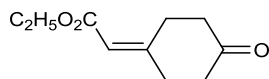
To a solution of 8-(bromomethylene)-1,4-dioxaspiro[4.5]decane (**S2**) (1.70 g, 7.29 mmol) in tetrahydrofuran (80 mL), 10% aqueous HCl (40 mL) was added and the mixture stirred for 19 h. To the solution ethyl acetate (100 mL) and water (100 mL) were added and the organic phase separated. Aqueous phase was twice extracted and then the combined organic extracts were washed with water, dried over anhydrous Na_2SO_4 and concentrated. The residue was subjected to column chromatography to afford compound **3b** as colorless oil (1.13 g, 82%). ($R_f=0.52$ ethyl acetate/petroleum ether=1:9); $^1\text{H NMR}$ (300 MHz, CDCl_3) $\delta=6.13$ (s, 1H, CHBr), 2.68 (m, 2H), 2.59 (m, 2H), 2.44 (m, 4H); $^{13}\text{C NMR}$ (75 MHz, CDCl_3) $\delta=210.17$ (CO), 140.03, 101.86, 40.32, 39.44, 32.29, 28.72; MS (70 eV, EI): m/z (%): 188, 190 [M] $^+$ (72); HRMS (APCI+) calcd for $\text{C}_7\text{H}_{10}\text{BrO}$ [$M+H$] $^+$: 188.9909, 190.9889; found: 188.9904, 190.9883.

Preparation of 4-benzylidenecyclohexanone (**3c**)



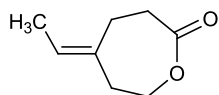
4-(Bromomethylene)cyclohexanone **3b** (108 mg, 0.57 mmol) and phenylboronic acid (84 mg, 0.68 mmol) were added in a 50 mL two necked round bottomed flask. Dioxane/ H_2O (4:1, 40 mL) was further added and solution flushed with nitrogen for 15 minutes, followed by the addition of K_2CO_3 (79 mg, 0.57 mmol). After addition of $\text{Pd}(\text{PPh}_3)_4$ (13.2 mg, 0.02% mol) and PPh_3 (3 mg, 0.02% mol), the solution was heated to 90 °C and refluxed for 24 hours when GC showed reaction completion. The mixture was rota-evaporated and the residue subjected to column chromatography to afford compound **3c** as a white solid (90 mg, 85%). ($R_f=0.36$ ethyl acetate/petroleum ether=1:9); $^1\text{H NMR}$ (300 MHz, CDCl_3) $\delta=7.29-7.14$ (m, 5H, H_{Ar}), 6.41 (s, 1H), 2.69 (m, 2H), 2.60 (m, 2H), 2.45 (m, 2H), 2.36 (m, 2H); $^{13}\text{C NMR}$ (75 MHz, CDCl_3) δ 211.38, 137.51, 137.32, 128.81, 128.38, 126.69, 125.78, 77.59, 77.16, 76.74, 41.58, 40.76, 34.85, 27.25; MS (70 eV, EI): m/z (%): 186 [M] $^+$ (100); HRMS (APCI+) calcd for $\text{C}_{13}\text{H}_{15}\text{O}$ [$M+H$] $^+$: 187.1117; found: 187.1118.

Preparation of ethyl 2-(4-oxocyclohexylidene)acetate (**3d**)



In a two necked round bottomed flask 4-(bromomethylene)cyclohexanone **3b** (301 mg, 1.59 mmol) and DIPEA (471 μ L, 2.71 mmol) were added to a mixture of dry ethanol and dry tetrahydrofuran (2:1, 30 mL) and the solution flushed with argon for 15 minutes. After this time Pd(PPh₃)₄ (55 mg, 0.03% mol) and PPh₃ (12.5 mg, 0.03% mol) were added and solution flushed for 5 additional minutes. A balloon filled with CO was then connected to the solution and a second one was attached to the installation equipped with condenser. The mixture was heated at 70 °C and after 24 hours GC indicated the total conversion of the starting material. The reaction mixture was rota-evaporated and the residue charged on a chromatographic column to afford (**3d**) as a pale yellow solid (160 mg, 55%). (*R*_f=0.41 ethyl acetate/petroleum ether=1:4); ¹H NMR (300 MHz, CDCl₃) δ = 5.78 (s, 1H), 4.10 (q, ³*J*=7.1 Hz, 2H), 3.13 (m, 2H), 2.58 (m, 2H), 2.44 (m, 6H), 1.23 (t, ³*J*=7.1 Hz, 3H); ¹³C NMR (75 MHz, CDCl₃) δ = 210.21, 166.14, 156.71, 116.19, 59.89, 39.58, 39.00, 33.85, 26.79, 14.28 ppm; HRMS (EI): calcd for C₁₀H₁₄O₃ [*M*]⁻: 182.0937; found: 182.0943.

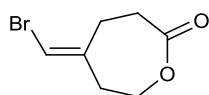
Preparation of (*E*)-4-ethylidene- ϵ -caprolactone (*E*-4a)



Method A. Using the general biotransformation procedure, WT-CHMO and 4-ethylidenecyclohexanone **3a** (0.283 g, 1.5 mmol) afforded (*E*-4a) as a white solid (0.137 g, 65%); *E/Z* = 98:2.

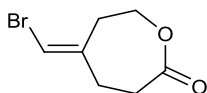
Method B. (*E*)-4-bromomethylene- ϵ -caprolactone (*E*-4b) (60 mg, 0.29 mmol) and methylboronic acid (23 mg, 0.38 mmol) were added in a 50 mL two necked round bottomed flask. Dry tetrahydrofuran (25 mL) was further added and solution degassed with argon for 15 minutes, followed by the addition of CsF (89 mg, 0.58 mmol). After addition of Pd(PPh₃)₄ (13.5 mg, 0.04% mol) and PPh₃ (3 mg, 0.04% mol) the solution was heated to 70 °C and refluxed for 24 hours when TLC showed reaction completion. The solution was rota-evaporated and the residue subjected to column chromatography to afford compound *E*-4a as a white solid (35 mg, 85%). (*R*_f=0.68 ethyl acetate/petroleum ether=1:1); ¹H NMR (400 MHz, CDCl₃) δ =5.24 (q, ³*J*=6.8 Hz, 1H), 4.11 (m, 2H), 2.54 (m, 2H), 2.39 (m, 2H), 2.33 (m, 2H), 1.53 (d, ³*J*=6.8 Hz, 3H); ¹³C NMR (101 MHz, CDCl₃) δ =175.56, 136.00, 121.34, 68.77, 39.71, 33.35, 24.00, 12.62; MS (70 eV, EI): *m/z* (%): 140 [*M*]⁺ (51); HRMS (APCI+) calcd for C₈H₁₃O₂ [*M+H*]⁺: 141.0910; found: 141.0909; *trans/cis* \geq 99:1.

Preparation of (*E*)-4-bromomethylene- ϵ -caprolactone (*E*-4b)



Using the general biotransformation procedure WT-CHMO and 4-bromomethylenecyclohexanone (**3b**) (0.283 g, 1.5 mmol) gave compound *E*-4b as a white solid (0.189 g, 62%). M.p. 91-93 °C; (*R*_f=0.40 ethyl acetate/petroleum ether=1:2); ¹H NMR (300 MHz, CDCl₃) δ =6.09 (s, 1H, CHBr), 4.22 (m, 2H), 2.63 (m, 6H); ¹³C NMR (75 MHz, CDCl₃) δ =174.71 (COO), 141.23, 103.96, 67.61, 38.41, 32.27, 27.39; MS (70 eV, EI): *m/z* (%): 204, 206 [*M*]⁺ (2); HRMS (APCI+) calcd for C₇H₁₀BrO₂ [*M+H*]⁺: 204.9858, 206.9838; found: 204.9857, 206.9837; *trans/cis* \geq 99:1.

Preparation of (Z)-4-bromomethylene- ϵ -caprolactone (Z-4b)



Using the general biotransformation procedure, mutant-CHMO and bromoketone **3b** (0.56 g, 1.5 mmol) gave compound (Z-4b) after two successive chromatographic columns as a white crystalline solid (0.042 g, 7%). (R_f = 0.40 ethyl acetate/petroleum ether=1:2); ^1H NMR (300 MHz, CDCl_3) δ =6.14 (s, 1H, CHBr), 4.25 (m, 2H), 2.79 (m, 2H), 2.68 (m, 2H), 2.50 (m, 2H); ^{13}C NMR (75 MHz, CDCl_3) δ =174.61, 141.19, 104.01, 67.09, 34.13, 33.33, 31.78; HRMS (APCI+) calcd for $\text{C}_7\text{H}_{10}\text{BrO}_2$ [$M+H$] $^+$: 204.9858, 206.9838; found: 204.9859, 206.9839.

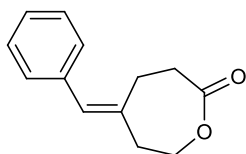
Diastereoisomers enrichment using column chromatography

The crude reaction product showed a *E/Z* ratio of 20:80 according to the GC analysis. First purification on column chromatography (ethyl acetate/petroleum ether=1:1) afforded a fraction containing the *E/Z* product (10:90 ratio) according to the GC analysis (126 mg, 21%). A second column chromatography (ethyl acetate/petroleum ether=1:2) afforded a fraction containing the *E/Z* product (1:99 ratio) according to the GC analysis (42 mg, 7%).

Diastereoisomers enrichment using HPLC

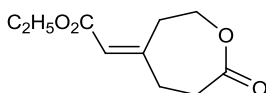
A mixture of *E/Z* lactone (112 mg, *E/Z* 23:87) dissolved in *i*-propanol (1.5 mL; final conc. 80.5 mg/mL) was loaded on a Shimadzu LC-8A HPLC and separated under the conditions mentioned below: Stationary Phase: LiChrospher Si 100 10 μm ; Column 250 x 20 mm BIA-X-Column, 95/17; Mobile Phase: *iso*-hexane/*iso*-propanol=95:5; Flow: 10.0 mL/min; Pressure: 0.2 MPa; Temperature 308 K; Detection UV, 210 nm, 0.2 mm. After separation, pure diastereoisomer *Z* (73 mg) was collected. 100% *Z*.

Preparation of (E)-4-benzylidene- ϵ -caprolactone (E-4c)



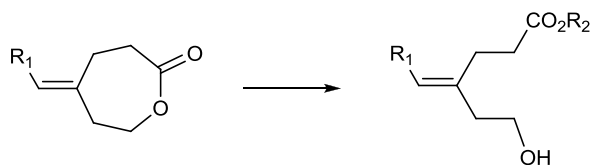
(*E*)-4-Bromomethylene- ϵ -caprolactone **E-4b** (46 mg, 0.22 mmol) and phenylboronic acid (33 mg, 0.26 mmol) were added in a 50 mL two necked round bottomed flask. Dry tetrahydrofuran (25 mL) was further added and the solution degassed with argon for 15 minutes, followed by the addition of CsF (68 mg, 0.44 mmol). After addition of $\text{Pd}(\text{PPh}_3)_4$ (10 mg, 0.04% mol) and PPh_3 (2 mg, 0.04% mol) the solution was heated to 70 $^\circ\text{C}$ and refluxed for 21 hours when GC showed reaction completion. The solution was rota-evaporated and the residue subjected to column chromatography to afford compound **E-4c** as a white solid (42 mg, 93%). (R_f =0.44 ethyl acetate/petroleum ether=1:2); ^1H NMR (300 MHz, CDCl_3) δ =7.18 (m, 5H, H_{Ar}), 6.35 (s, 1H, CHBr), 4.26 (m, 2H), 2.60 (m, 6H); ^{13}C NMR (75 MHz, CDCl_3) δ =175.47, 138.56, 136.89, 129.00 (2C), 128.50 (2C), 127.89, 127.02, 68.59, 40.26, 33.54, 25.47; MS (APCI) m/z : 203,1 [$M+H$] $^+$; HRMS (APCI+) calcd for $\text{C}_{13}\text{H}_{15}\text{O}_2$ [$M+H$] $^+$: 203.1067; found: 203.1065; *E/Z* \geq 99:1.

Preparation of ethyl (Z)-4-carboxymethylene- ϵ -caprolactone (Z-4d)



Using the general biotransformation procedure ketone **3d** (0.144 g, 0.79 mmol) and mutant CHMO gave after chromatographic chromatography compound **Z-4d** as a white solid (0.096 g, 61%). Initially the *Z/E* ratio was (96:4 in the favor of *Z*). After column chromatography two fractions were collected: one containing compound **Z-4d** (80 mg) (98:2 in the favor of *Z*) and the other one (16 mg) containing 87% *Z*. (R_f = 0.30 ethyl acetate/petroleum ether=1:1); ^1H NMR (300 MHz, CDCl_3) δ =5.77 (s, 1H, CHCO_2Et), 4.27 (m, 2H), 4.15 (q, $^3J=7.1$ Hz, 2H, $\text{CO}_2\text{CH}_2\text{CH}_3$), 3.31 (m, 2H), 2.71 (m, 2H), 2.50 (m, 2H), 1.28 (t, $^3J=7.1$ Hz, 3H, $\text{CO}_2\text{CH}_2\text{CH}_3$); ^{13}C NMR (75 MHz, CDCl_3) δ =174.60, 166.11, 156.40, 118.06, 67.34, 60.28, 33.94, 32.68, 32.12, 14.35; HRMS (ES+) calcd for $\text{C}_{10}\text{H}_{14}\text{O}_4\text{Na}$ [$M+H$] $^+$: 221.0784; found: 221.0784; *E/Z* 2.5:97.5.

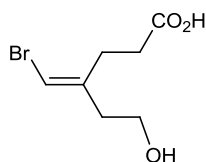
Lactones behavior in reaction with nucleophiles



$R_1=\text{Br}$; **E-4b**
 $R_1=\text{Ph}$; **E-4c**

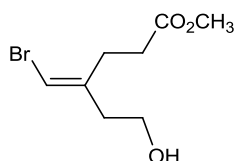
$R_1=\text{Br}$; $R_2=\text{H}$, **S3**
 $R_1=\text{Br}$; $R_2=\text{CH}_3$, **S4**
 $R_1=\text{Ph}$; $R_2=\text{H}$, **S5**

Preparation of (*E*)-4-(bromomethylene)-6-hydroxyhexanoic acid (**S3**)



To a stirred solution of bromolactone **E-4b** (41 mg, 0.2 mmol) in THF/ H_2O (8:1, 10 mL) Na_2CO_3 (53 mg, 0.5 mmol) was added and then the solution was heated at 70°C . The mixture was refluxed overnight, allowed to cool to r.t. and then NaOH solution (5 mL) was added followed by the addition of ethyl acetate (5 mL). The aqueous phase was separated, washed twice with ethyl acetate, then acidified to pH2 and extracted with ethyl acetate twice. The combined organic phases were washed with H_2O twice, dried over anhydrous Na_2SO_4 and evaporated to afford (*E*)-4-(bromomethylene)-6-hydroxyhexanoic acid (**S3**) as a colorless oil (37 mg, 83%). (R_f =0.32 ethyl acetate); ^1H NMR (300 MHz, CDCl_3) δ =6.54 (broad s, 2H, COOH , OH), 6.03 (s, 1H, CHBr), 3.69 (t, $^3J=6.1$ Hz, 2H, CH_2OH), 2.51-2.34 (m, 6H); ^{13}C NMR (75 MHz, CDCl_3) δ =178.24 (COOH), 140.37, 105.36, 60.42, 39.07, 31.48, 28.07; MS (APCI+) m/z : 222.1, 223.0 [$M+H$] $^+$; HRMS (APCI-): calcd for $\text{C}_7\text{H}_{10}\text{BrO}_3$ [$M-H$] $^-$: 220.9807, 222.9788; found: 220.9819, 222.9798.

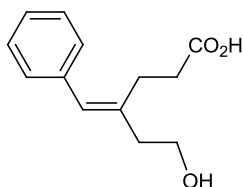
Preparation of (*E*)-methyl 4-(bromomethylene)-6-hydroxyhexanoate (**S4**)



(*E*)-4-Bromomethylene- ϵ -caprolactone **E-4b** (44 mg, 0.21 mmol) and DIPEA (37 μL , 0.21 mmol) were added in a 25 mL two necked round bottomed flask filled with methanol (25 mL). The mixture was then refluxed to 75°C for 2 hours when TLC showed reaction completion. The reaction

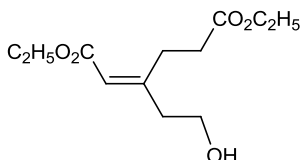
mixture was rota-evaporated and the residue subjected to column chromatography to afford compound **S4** as colorless oil (42 mg, 88%). ($R_f=0.40$ ethyl acetate/petroleum ether=1:1); $^1\text{H NMR}$ (300 MHz, CDCl_3) $\delta=6.05$ (s, 1H), 3.69 (m, 5H, CH_2OH , COOCH_3), 2.44 (m, 6H). $^{13}\text{C NMR}$ (75 MHz, CDCl_3) $\delta=173.37$ (COOCH_3), 140.66, 104.87, 60.28, 51.92, 39.15, 31.54, 28.31. MS (APCI+) m/z : 237.2 [$M+H$] $^+$; HRMS: calcd for $\text{C}_8\text{H}_{14}\text{BrO}_3$: [$M+H$] $^+$: 237.0121, 239.0101; found: 237.0120, 239.0099.

Preparation of (*E*)-4-benzylidene-6-hydroxyhexanoic acid (**S5**)



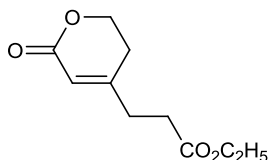
(*E*)-4-Bromomethylene- ϵ -caprolactone **E-4b** (40 mg, 0.19 mmol) and phenylboronic acid (29 mg, 0.23 mmol) were added in a 50 mL two necked round bottomed flask. Dioxane/ H_2O (4:1, 25 mL) was further added and solution degassed with nitrogen for 15 minutes, followed by the addition of K_2CO_3 (54 mg, 0.39 mmol). After addition of $\text{Pd}(\text{PPh}_3)_4$ (3 mg, 0.02% mol) the solution was heated to 70 °C and refluxed for 24 hours when GC showed reaction completion. The solution was rota-evaporated and the residue subjected to column chromatography to afford compound **S5** as colorless liquid (34 mg, 86%). ($R_f=0.60$ methanol/ethyl acetate=1:8); $^1\text{H NMR}$ (300 MHz, $\text{DMSO}-d_6$) $\delta=7.23$ (m, 5H, H_{Ar}), 6.24 (s, 1H, CHBr), 3.56 (t, $^3J=7.0$ Hz, 2H, CH_2OH), 2.51-2.07 (m, 6H); $^{13}\text{C NMR}$ (75 MHz, $\text{DMSO}-d_6$) $\delta=177.87$ (COOH), 140.35, 137.72, 128.31 (2C), 128.14 (2C), 125.98, 125.92, 60.03, 40.10, 34.97, 27.22; MS (ES+) m/z : 243.0 [$M+\text{Na}$] $^+$; HRMS (APCI-): calcd for $\text{C}_{13}\text{H}_{15}\text{O}_3$ [$M-H$] $^-$: 219.1027; found: 219.1024.

Preparation of (*E*)-diethyl 3-(2-hydroxyethyl)hex-2-enedioate (**E-5**)



In a two necked round bottomed flask, (*E*)-4-bromomethylene- ϵ -caprolactone **E-4b** (63 mg, 0.30 mmol) and absolute EtOH (35 mL) were added and the solution flushed with argon for 15 minutes. After this time $\text{Pd}(\text{PPh}_3)_4$ (14 mg, 0.05% mol), PPh_3 (3 mg, 0.04% mol) and CsF (93 mg, 0.61 mmol) were added and the solution flushed with argons for 5 additional minutes. A balloon filled with CO was then connected to the solution for 10 minutes and a second one was attached to the installation equipped with condenser. The mixture was heated at 80 °C and refluxed for 48 hours when GC indicated the total conversion of the starting material. The reaction mixture was rota-evaporated and the residue charged on a chromatographic column to afford **E-5** as colorless oil (46 mg, 61%). ($R_f=0.47$ ethyl acetate/petroleum ether=1:1); $^1\text{H NMR}$ (300 MHz, CDCl_3) $\delta=5.76$ (s, 1H), 4.14 (m, 4H), 3.79 (t, $^3J=6.3$ Hz, 2H), 2.89 (m, 2H), 2.51 (m, 2H), 2.42 (td, $^3J=6.3$ Hz, $^4J=1.0$ Hz, 2H), 1.80 (s, 1H), 1.25 (dt, $^3J=7.1$ Hz, 6H); $^{13}\text{C NMR}$ (75 MHz, CDCl_3) $\delta=173.11$, 165.95, 158.08, 118.88, 60.71, 60.49, 59.98, 41.48, 33.00, 27.68, 14.38, 14.33; MS (APCI+) m/z : 245.0 [$M+H$] $^+$; HRMS (APCI+): calcd for $\text{C}_{12}\text{H}_{21}\text{O}_5$ [$M+H$] $^+$: 245.1384; found: 245.1376.

Preparation of ethyl 3-(6-oxo-3,6-dihydro-2H-pyran-4-yl)propanoate (6)



Method A

Compound Z-4d (24 mg, 0.12 mmol) was added in absolute ethanol (5 mL) into a 10 mL round bottomed flask and the mixture refluxed at 80 °C. The reaction was monitored on GC and after completion (aprox. 2 h) the solution was evaporated to dryness to afford compound 6 as a colorless liquid. Additionally to the initial mixture DIPEA can be added in catalytic traces to speed up the reaction time (24 mg, quant). ($R_f=0.37$ ethyl acetate/petroleum ether=1:1); $^1\text{H NMR}$ (300 MHz, CDCl_3) $\delta=5.79$ (t, $^4J=1.4$ Hz, 1H), 4.37 (t, $^3J=6.2$ Hz, 2H), 4.14 (q, $^3J=7.1$, 2H), 2.56 (m, 4H), 2.41 (t, $^3J=6.2$ Hz, 2H), 1.26 (t, $^3J=7.1$, 3H); $^{13}\text{C NMR}$ (75 MHz, CDCl_3) $\delta=172.01$, 164.43, 159.48, 116.17, 66.02, 61.05, 31.41, 31.13, 28.22, 14.33; HRMS (ES+): calcd for $\text{C}_{10}\text{H}_{14}\text{O}_4\text{Na}$ [$M+\text{Na}$] $^+$: 221.0784; found: 221.0785.

Method B

In a two necked round bottomed flask bromolactone Z-4b (16 mg, 78 μmol) and CsF (35 mg, 0.234 mmol) were added to a mixture of dry ethanol and dry tetrahydrofuran (4:1, 15 mL) and the solution flushed with argon for 15 minutes. After this time $\text{Pd}(\text{PPh}_3)_4$ (5 mg, 0.05% mol) and PPh_3 (1 mg, 0.05% mol) were added and solution flushed for 5 additional minutes. A balloon filled with CO was then connected to the solution and a second one was attached to the installation equipped with condenser. The mixture was heated at 80 °C and after 48 hours GC indicated the total conversion of the starting material. The reaction mixture was rota-evaporated and the residue charged on a chromatographic column to afford compound 6 as a colorless liquid (12 mg, 78%).

QM/MM calculations

Starting from the Criegee intermediate structure containing cyclohexanone (obtained from Polyak et al. 2012²) the two 4-ethylidene-cyclohexanone-containing Criegee intermediates that would lead to the *Z*- and *E*-lactone products were built manually. The resulting structures were subjected to the QM/MM optimizations using the ChemShell program³ and the HDLCopt⁴ optimizer. The TURBOMOLE program⁵ was used to obtain the energy and gradients for the QM part using the density functional theory (employing the B3LYP functional^{6,7,8,9,10,11} and the TZVP basis set¹²) and the DL_POLY program¹³ was employed to compute the energy and gradients of the MM part represented by the CHARMM22 force field.¹⁴ The QM region is analogous to the one used in Polyak et al, 2012,²² containing all atoms from the isoalloxazine ring of C4a-peroxyflavin, the 4-ethylidene-cyclohexanone, the side chain of Arg329, and the nicotineamide ring and the adjacent ribose of NADP⁺. The QM atoms and all the MM atoms within 12 Å of the C4a atom in the isoalloxazine ring of FADHOO- were allowed to freely move during the optimization.

During the two optimizations both Criegee intermediates remained stable and only minor conformational changes in the binding site occurred. The two optimized structures differed in the QM(B3LYP/TZVP)/CHARMM energy by 2.3 kcal/mol, with the one containing the 4-ethylidene-cyclohexanone that would lead to formation of the *E*-lactone product being energetically favored. In the other pose (that would lead to the *Z*-lactone product) in its original non-optimized configuration the ethylidene group appears to be too close to the backbone of amino acids 434-435, lining the binding pocket. During optimization the 4-ethylidene-cyclohexanone therefore had to perform larger displacement from the initial configuration, and, although the Criegee intermediate remained stable, it leads to the less energetically favorable configuration.

MM calculations

Choosing appropriate randomization sites for iterative saturation mutagenesis (ISM) and initial MM analysis

In order to choose feasible sites for randomization in the process of iterative saturation mutagenesis, the X-ray data of the homologous CHMO from *Rhodococcus*¹⁵ as a theoretical structural model of CHMO from *Acinetobacter* sp. NCIMB 98 was used as a guide. This model appears to be a good starting point to study the observed phenomenon in CHMO. The whole amino acid sequence possesses about 75% identity and 85% positives with the CHMO from *Acinetobacter* (positive refers to similar amino acids), and all amino acids within 10 Å from the substrate binding site have 95% identity and 100% positives. To rationalize the choice of randomization sites for ISM, and to unveil the source of *E*-diastereoselectivity in the case of CHMO wild type (WT) using 4-ethylidenecyclohexanone (**3a**), the reactant complex was constructed. The initial structural template for the reactant complex was obtained from a previous QM/MM study² using cyclohexanone and the X-ray structure of CHMO from *Rhodococcus* sp. strain HI-31.

For docking of 4-ethylidenecyclohexanone (**3a**) into the CHMO binding site, cyclohexanone was removed from the reactant complex in the template and 4-ethylidenecyclohexanone was docked using the Glide software^{16,17,18}. Docking poses were analyzed and most of the aligned substrates placed the 4-ethylidene group in an orientation that leads to the *E*-**4a** formation (*E*-binding mode); following the corresponding Criegee-intermediate formation, anti-periplanar arrangement and σ -bond migration. The best docking result shows an *E*-binding mode and a docking score of -5.105 kcal/mol (Fig. S1) and the best obtained pose leading possibly to a *Z*-configuration product has a score of -3.890 kcal/mol. In both cases the key distances in the reactant complex were comparable to the distances reported previously for cyclohexanone². For example, the distance between the carbonyl oxygen atom of the substrate and the nearest Arg329 NH hydrogen is 1.5 Å (1.735 Å for the *Z* leading pose), and the distance between the C1 carbon of the carbonyl group from the substrate and the negatively charge oxygen of the peroxyflavin intermediate (FADHOO⁻) is 3.16 Å (3.2 Å for the *Z* leading pose).

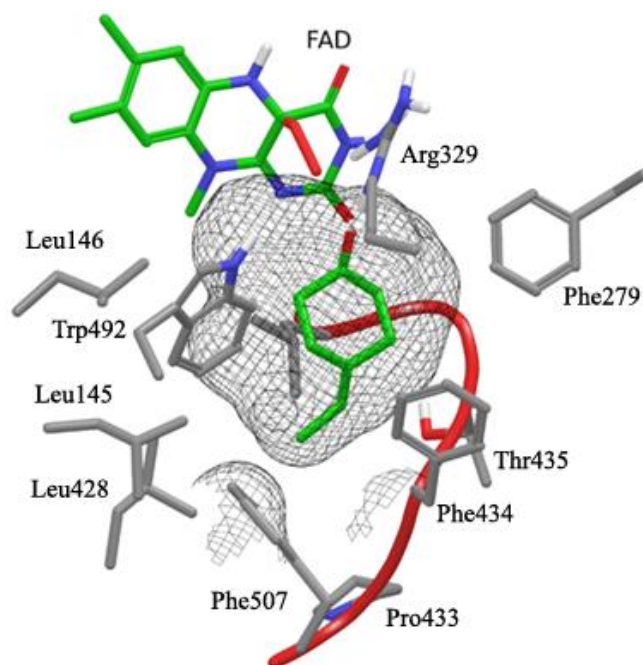


Figure S1 | Scheme of the reactant complex in the *E*-selective WT CHMO. The favored reactant complex which produces the *E*-lactone is shown in green together with the riboflavin moiety. The formation of *Z*-lactone derived from the respective reactant complex (methyl group in the corresponding ethylidene pointing to the red loop, not shown) is most likely restricted by steric effects from the amino acids located in the loop 433-436 (marked in red).

In the Polyak et al work², it was shown how the reaction proceeds in the active site, the anti-periplanar arrangement of C-C-O-O being one of the requirements for smooth cleavage (fragmentation) of the Criegee intermediate. The authors affirmed that once the Criegee-intermediate is formed, there is only one possible σ -bond migration due to the stereoelectronic requirement. This implies that the energetically preferred binding mode of cyclohexanone sets the stage for all subsequent molecular events. In other words, if a substrate is able to correctly dock into the binding site and energetically capable of forming a Criegee-intermediate having an anti-periplanar C-C-O-O arrangement, then an ester or lactone will be formed. The produced isomer is determined previously by the substrate binding mode, which at the same time depends on the environmental molecular relation between the substrate and the binding sites (H-bond, hydrophobic and electrostatic interactions, steric effects, etc.). According to the docking studies, it can be concluded that *Z*-**4a** product formation is mainly hampered by steric effects generated from the loop 431-434, whereas the preferred *E*-binding mode in the active site is energetically favored and not influenced adversely by possible clashes with other residues. The *E* and *Z*-configuration in the final product is determined by the most favored positional orientation of the 4-ethylidene group in the binding site, which is reflected by a better binding score. This orientation could be left or right (*E* or *Z* respectively) in Fig. S1 (only the *E*-binding mode is shown).

This partial theoretical explanation for *E*-selectivity provided some hints for choosing the CAST randomization sites and routing for the ISM experiments. For a limited number of ISM experiments, one possible ISM pathway was chosen. This pathway considers the double residue site A (positions 434 and 435) and single residue sites B (position 145) as well as C (position 507) (**Figure S1**). The pathway followed the randomization in an A, B and C order.

Basically, the ISM strategy followed first the generation of permissive mutations to allow the binding mode that leads to the corresponding *Z*-**4a** formation and afterward mutations that would block the binding mode for *E*-**4a** formation. This procedure would lead hypothetically to the progressive shifting in diastereoselectivity. Although laboratory evolution is rarely predicted in a precise way, this rational way to choose the randomization sites for CASTing is expected to increase the chances of success.

The first round of mutation was intended to increase the space in the region of loop 433-436, the main identified steric element that favors *E*-configuration at the expense of the *Z*-mode. For this purpose, positions 434 and 435 were chosen. Later on, residues presumably capable of blocking the *E*-binding mode were proposed, and residues 145 and 507 appeared to be at right position and distance for this goal (Fig. S1). At this point, the possible optimal mutations can be expected to have large enough side chains to disfavor the 4-ethylidene orientation that results in a *E*-**4a** formation, but not too large to block the alternative substrate alignment that generates the *Z*-**4a** lactone.

Analysis of the Criegee-intermediates leading to *E*- or *Z*-lactone formation

The two possible Criegee-intermediates producing either the *E* or *Z* configured lactone were analyzed (Fig. S2). To build this intermediate, the ethylidene group at position 4 in the Criegee intermediate of cyclohexanone previously optimized at a QM(B3LYP/TZVP)/CHARMM level² was added manually.

Energy and MD minimization were applied to adjust the new position of residues in the active site. Because the stereo-electronic requirement for the Criegee intermediate to proceed in the BV reaction comprises an anti-periplanar rearrangement with the FADO:OX3-OX3'-CYHN:C1-C2 dihedral angle being close to 180° (consult reference 2), our MD simulation for the two possible Criegee-intermediates were performed constraining such dihedral angle close to 180°. 10 ns of productive simulation was obtained using the Desmond program and OPLS-AA force field^{19,20,21}. The MD simulations used the SPC water solvent system^{22,23} including a concentration of 150 mM NaCl. Partial atomic charges of the 4-ethylidencyclohexanone in the Criegee-intermediate were calculated using the Jaguar application¹⁸ (electrostatic potential fitting) to improve the representation of molecular electrostatic potential. These parameters were included in the force field used for the MD simulations. Long-range electrostatic interactions using Particle Mesh Ewald

(PME) and van der Waals interactions were computed with a real space contributions truncated at 9 Å. Bond lengths to hydrogens were constrained by using the SHAKE algorithm. A RESPA integrator was used with time steps set to 2 fs for bonded and short-range nonbonded interactions, and 6 fs for long-range electrostatic interactions. Prior to every dynamic simulation, the solvated systems were relaxed into a local energy minimum using 500 steps of a hybrid method of steepest descent minimization and a limited-memory Broyden-Fletcher-Goldfarb-Shanno (L-BFGS) minimization. Additionally before simulation, the model systems were relaxed through a series of minimization and short dynamic simulations (NPT ensemble using a Berendsen thermostat and barostat) equilibrating the system at 300 K and 1 atm. Finally, production simulations were performed for every solvated system during 10 ns, coupling the system using NPT simulation, maintaining 1 atm at 300 K with a Martyna–Tobias–Klein barostat (relaxation time of 2 ps) and a Nose–Hoover thermostat (relaxation time of 0.5 ps). The difference in the total potential energy in the whole enzyme/Criegee-intermediate complex between the *E* and *Z* configuration using the opls-2005 force field was 1883 KJ/mol (450 kcal/mol), favoring the *E* configuration.

The corresponding Criegee-intermediate for the *Z* formation is less energetically favored compared to the *E* configuration. This effect and the preferred binding mode is explained basically by the restricted space in the active site, where the substrate orientation is sterically arranged to a reactant complex which would consecutively produce the corresponding *E* product.

After manually forcing the *Z* arrangement into the Criegee-intermediate, and after minimizing the structure, it becomes clear that a notable global structural arrangement is necessary to harbor such intermediates into the active site compared to the *E* pose, especially at the loop 433-436, which would explain the big differences in terms of potential energy. RMSD values between the template Criegee-intermediate (QM/MM optimized intermediate²) and the corresponding *E* and *Z* intermediate including only the residues within 7 Å from the substrate proved to be 1 Å larger for the *Z* configuration, reflecting the major protein rearrangement in the *Z* case.

As already mentioned, a QM/MM study of CHMO-catalyzed desymmetrization of 4-methylcyclohexanone sheds light on the origin of this type of stereoselectivity, the energetic difference between this substrate with methyl in the equatorial versus axial orientation determining the degree of enantioselectivity². In the present case of substrate **3a**, the molecule is more flexible and the equatorial/axial issue is not relevant. Nevertheless, the two possible orientations of the 4-ethylidene in the substrate direct the final diastereoselectivity. The *E* and *Z* configuration in the final product is determined by the most favored positional orientation of the 4-ethylidene group in the binding site, which is reflected by a better binding score and more stable Criegee-intermediate. This orientation could be left or right in Fig. S2 (*E* and *Z* respectively). Thus, the present MM analysis leads qualitatively to the same model as the more refined QM/MM approach described above.

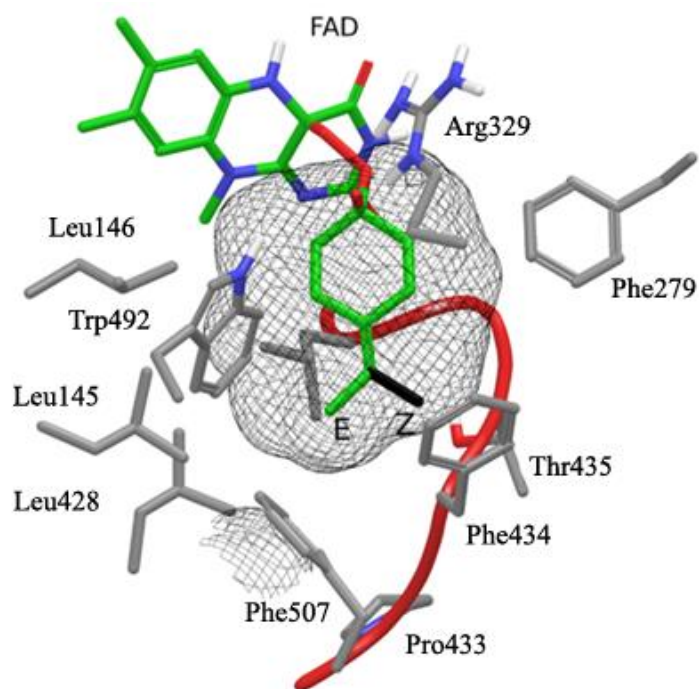
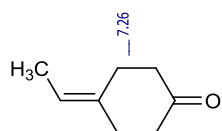


Figure S2 | Scheme of the Criegee-intermediate in the *E*-selective WT CHMO. The favored Criegee-intermediate which produces the *E*-lactone is shown in green together with the riboflavin moiety. The intermediate going to the *Z*-lactone is represented with a black methyl group in the corresponding ethylidene. The formation of the *Z*-isomer is clearly restricted by the amino acids located in the loop 433-436 (marked in red).

NMR spectra

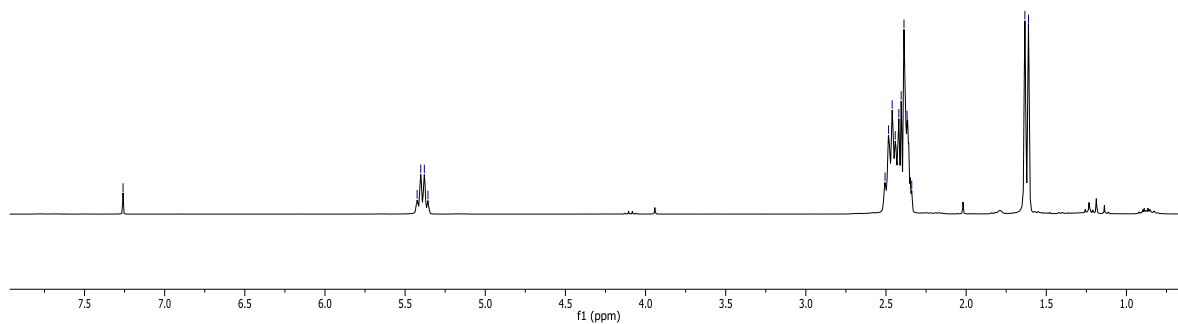
^1H NMR (300 MHz, CDCl_3) and ^{13}C NMR (75 MHz, CDCl_3) spectra of compound 3a



5.43
5.40
5.38
5.36

2.51
2.48
2.46
2.44
2.42
2.41
2.39
2.37
2.34

1.63
1.61



212.01

134.63

119.48

77.59 CDCl_3
77.16 CDCl_3
76.74 CDCl_3

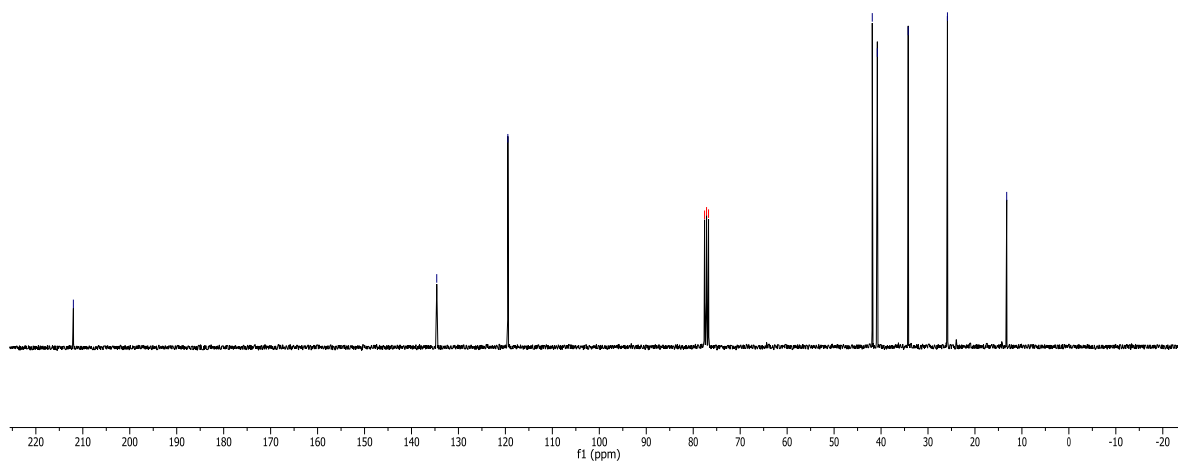
41.87

40.79

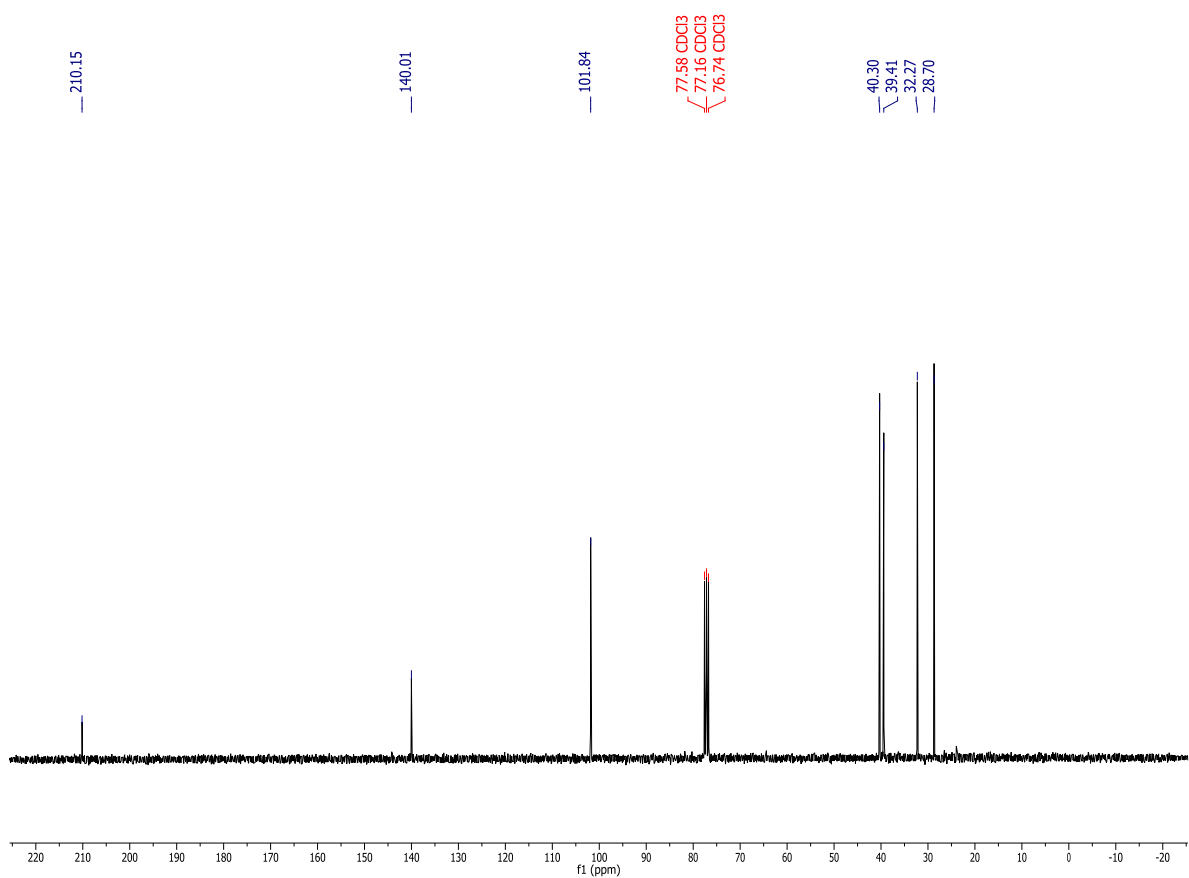
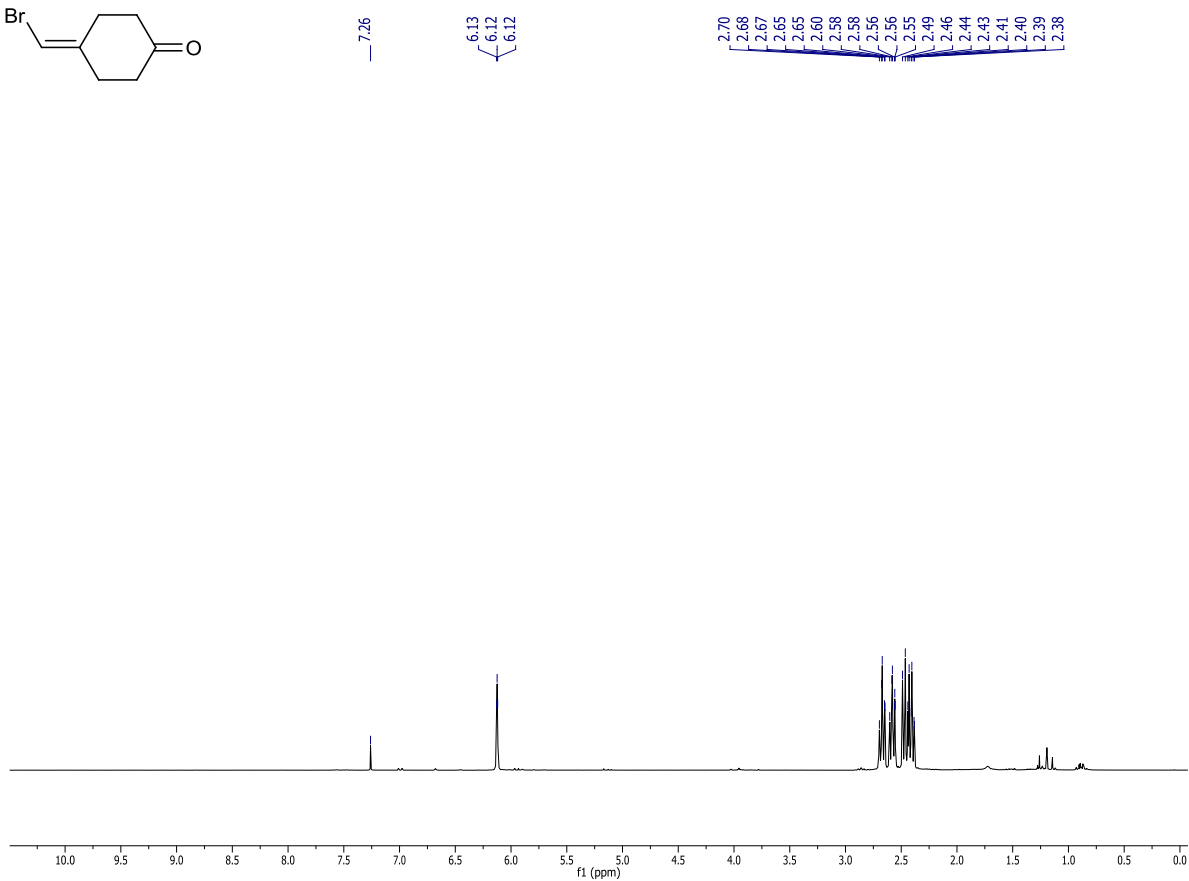
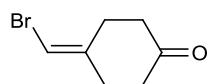
34.22

25.86

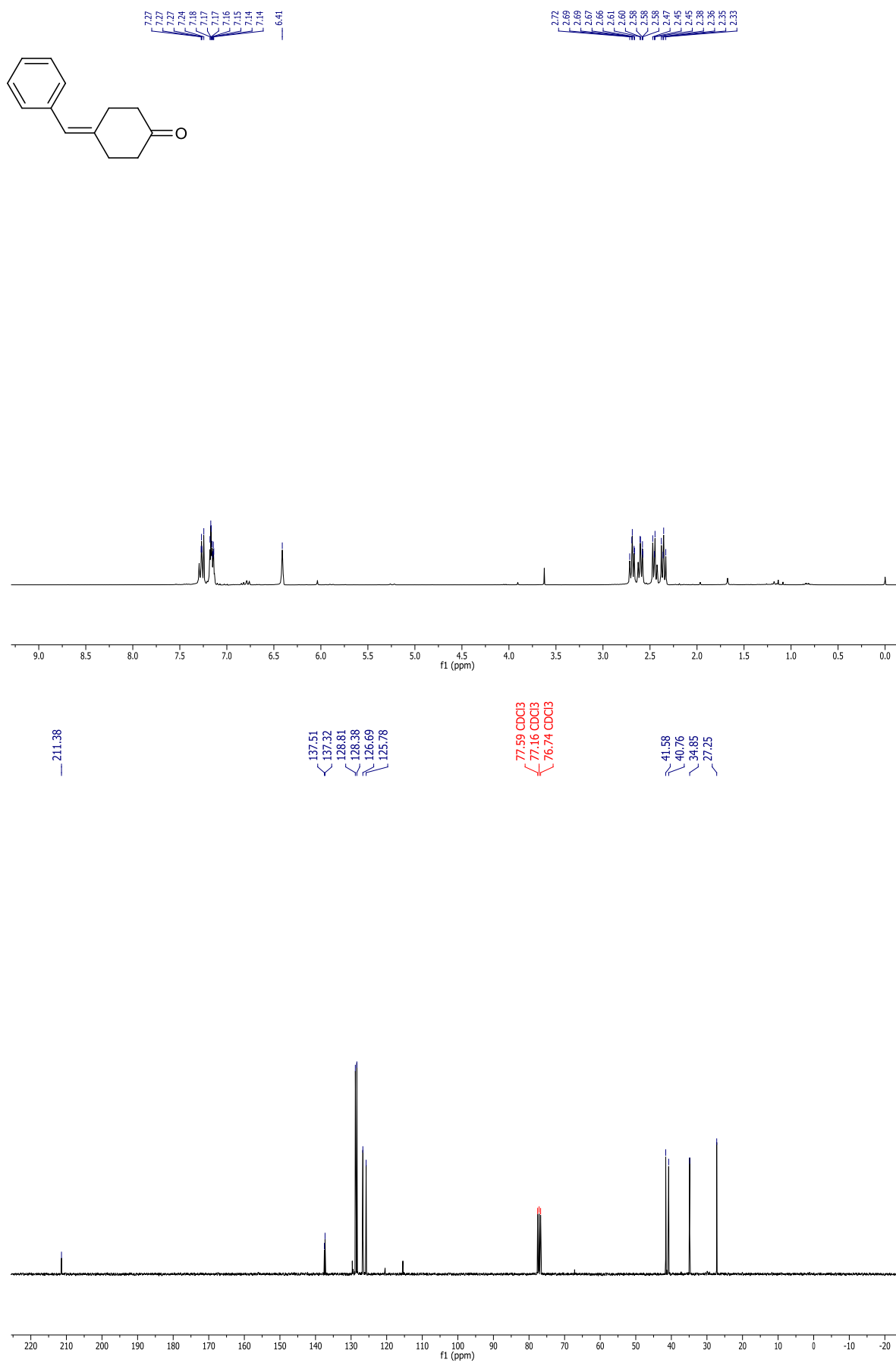
13.24



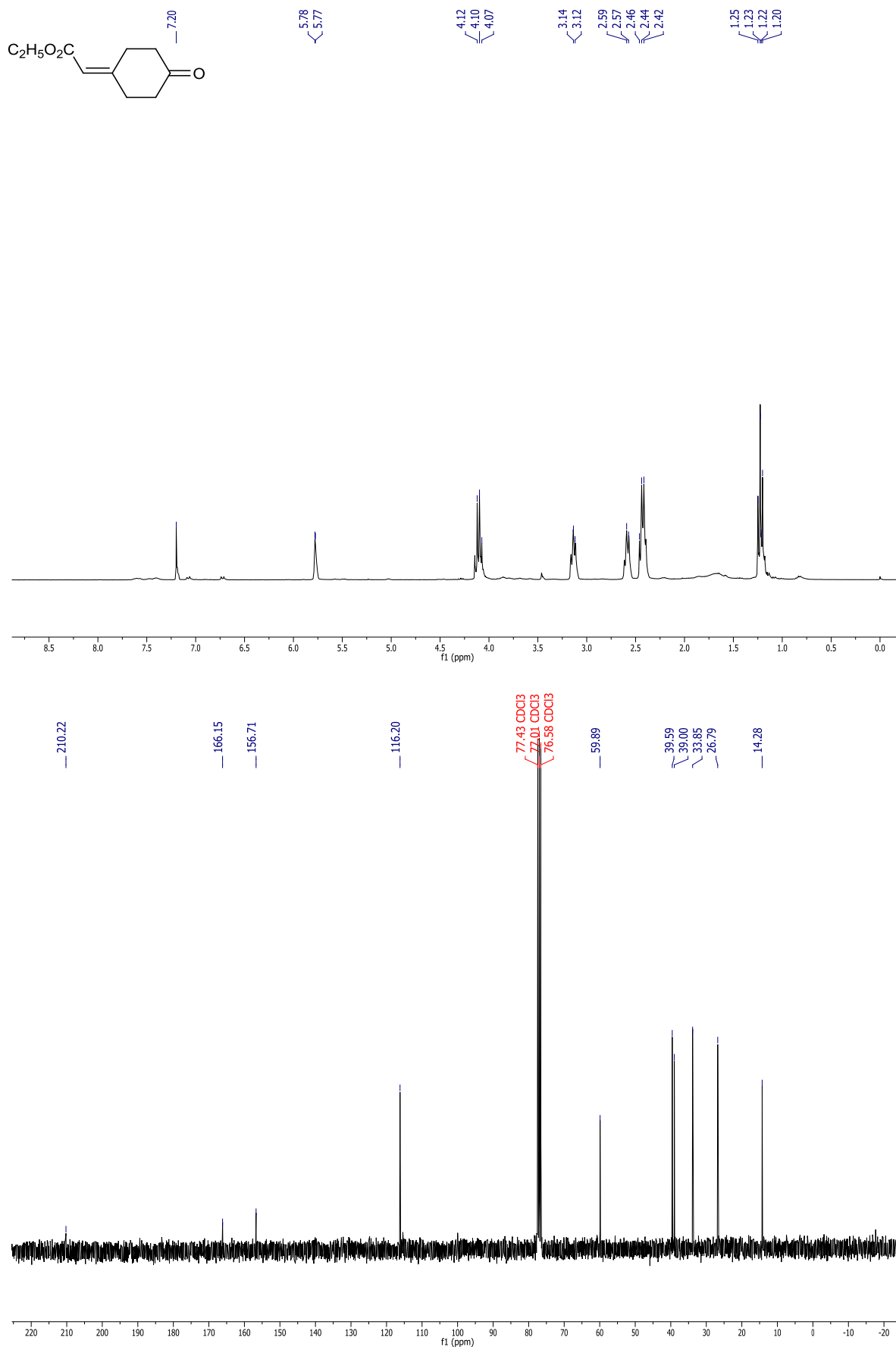
^1H NMR (300 MHz, CDCl_3) and ^{13}C NMR (75 MHz, CDCl_3) spectra of compound 3b



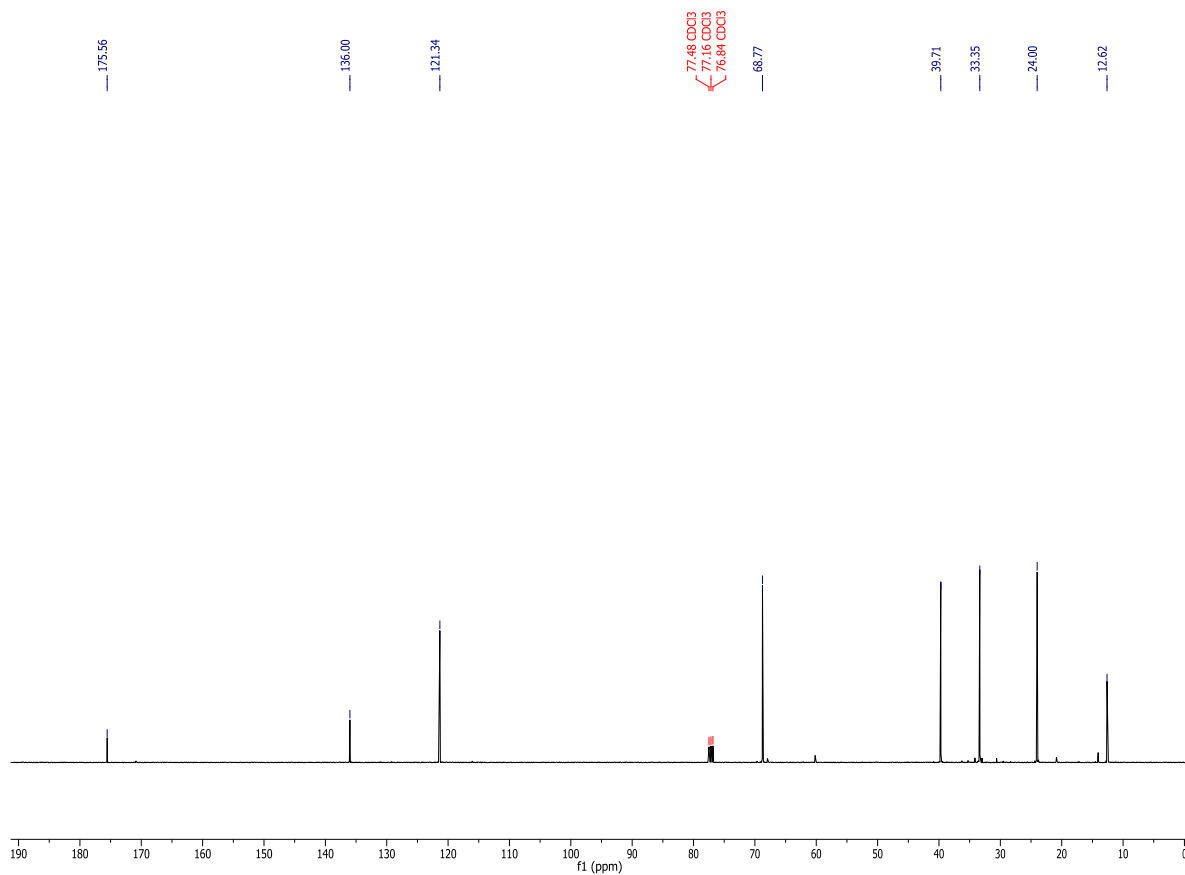
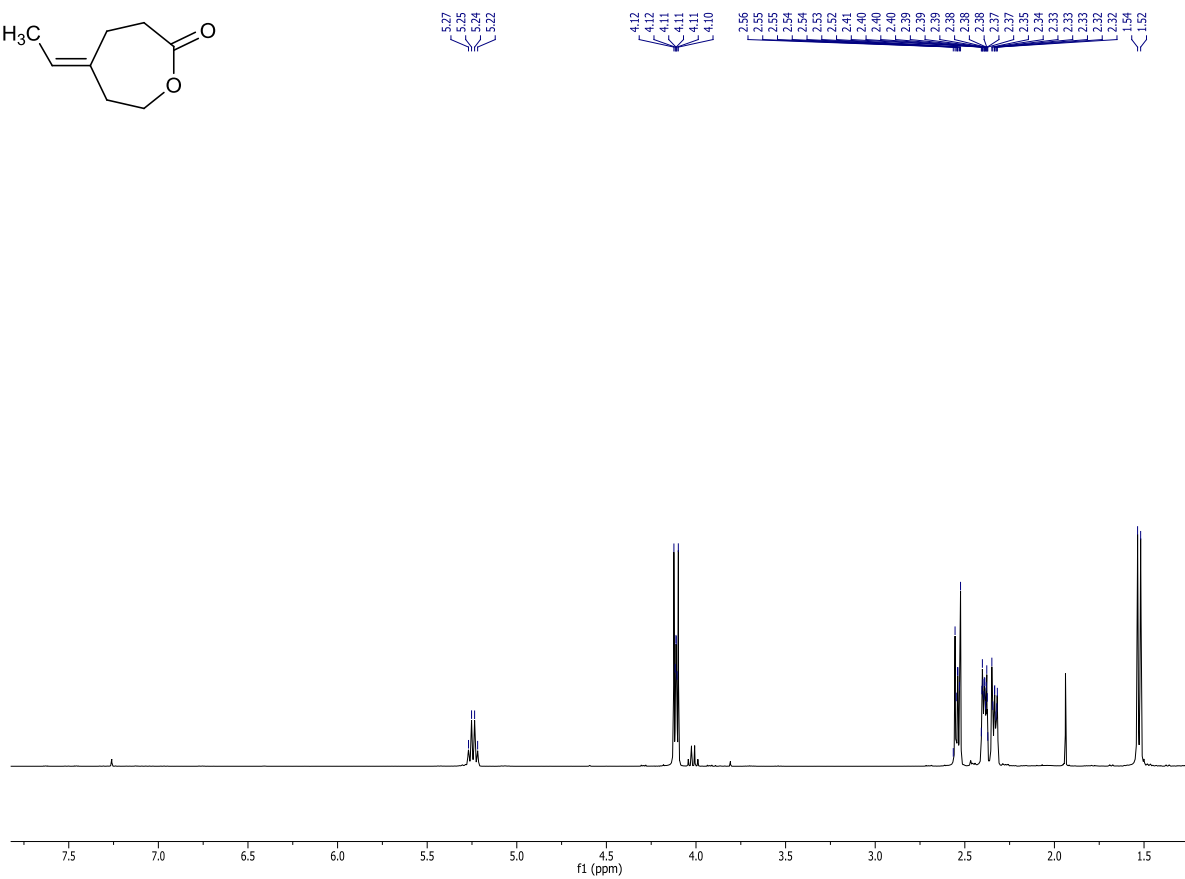
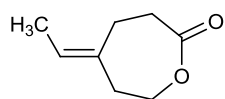
^1H NMR (300 MHz, CDCl_3) and ^{13}C NMR (75 MHz, CDCl_3) spectra of compound 3c



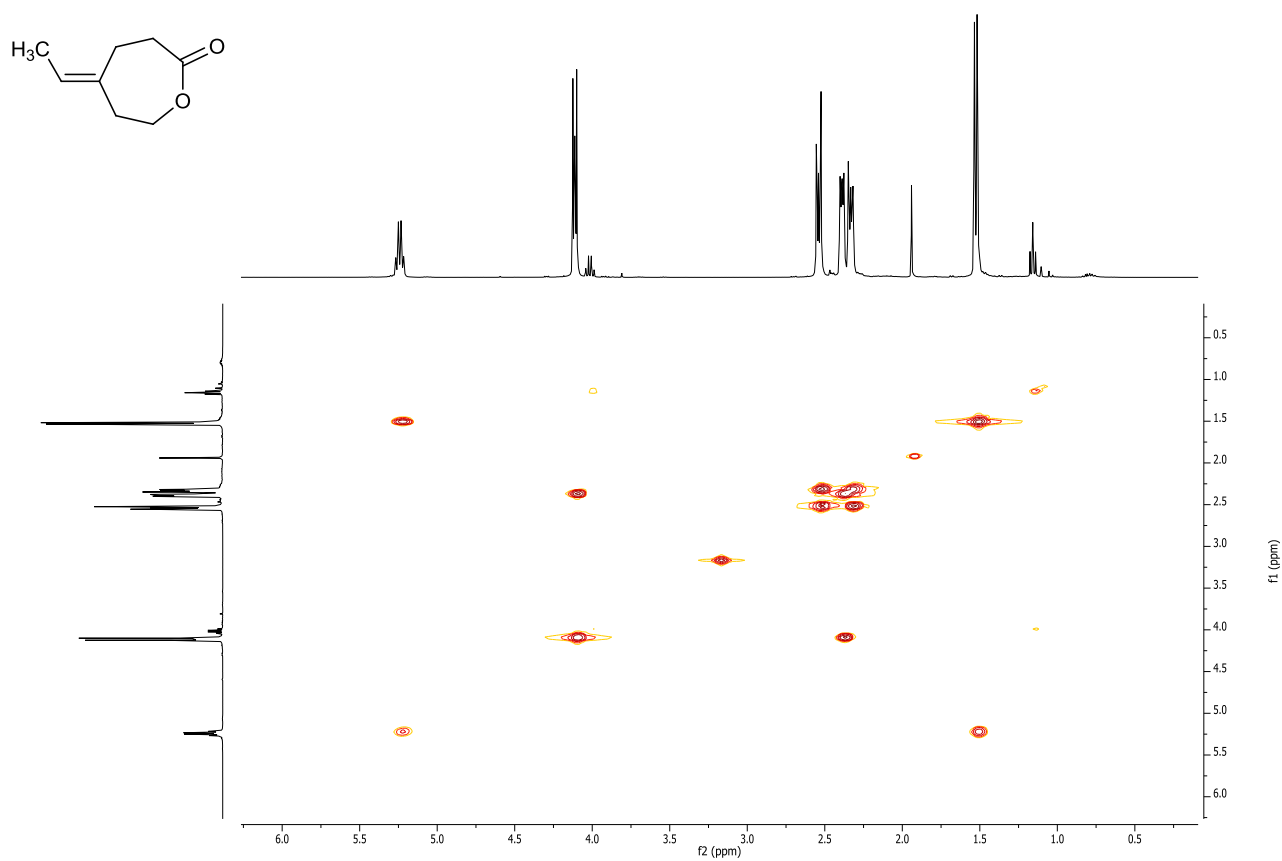
^1H NMR (300 MHz, CDCl_3) and ^{13}C NMR (75 MHz, CDCl_3) spectra of compound 3d



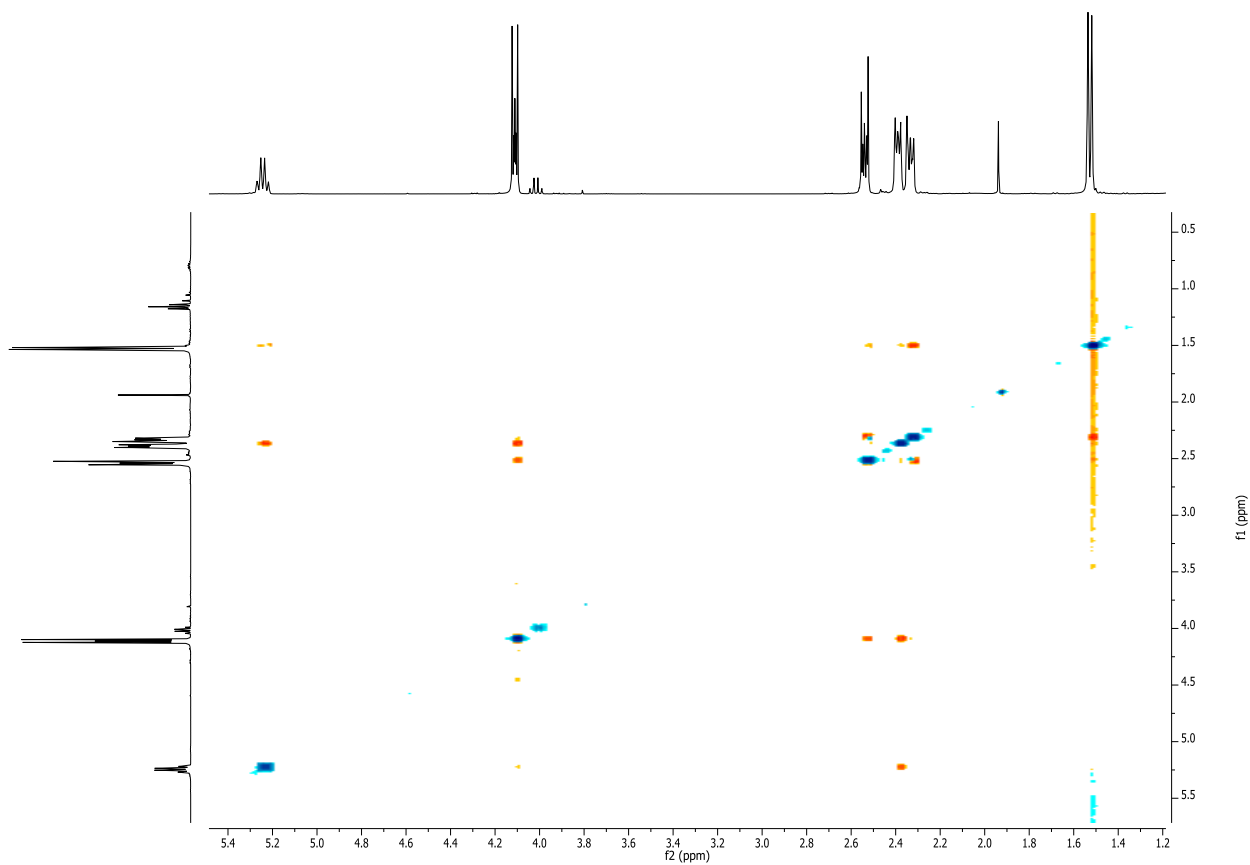
^1H NMR (400 MHz, CDCl_3) and ^{13}C NMR (101 MHz, CDCl_3) spectra of compound *E*-4a



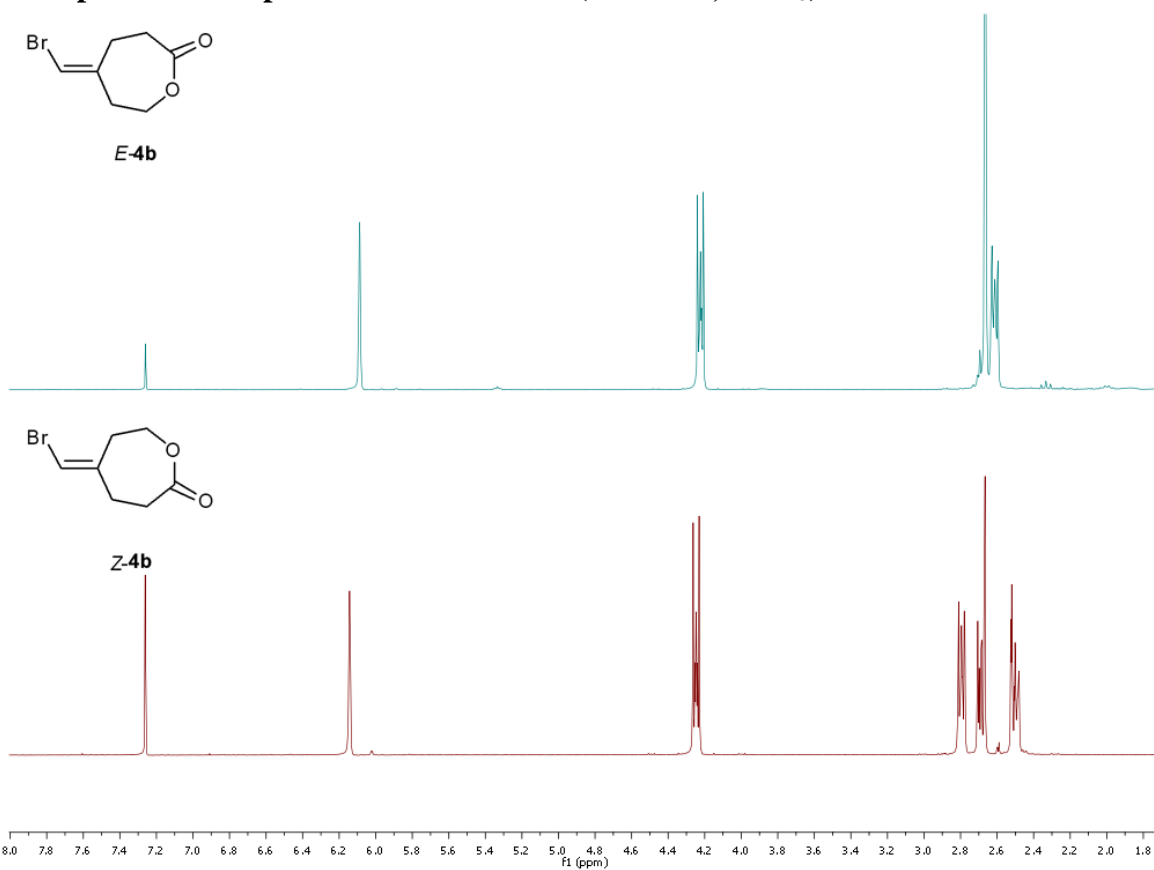
COSY spectrum of compound *E*-4a (CDCl₃)



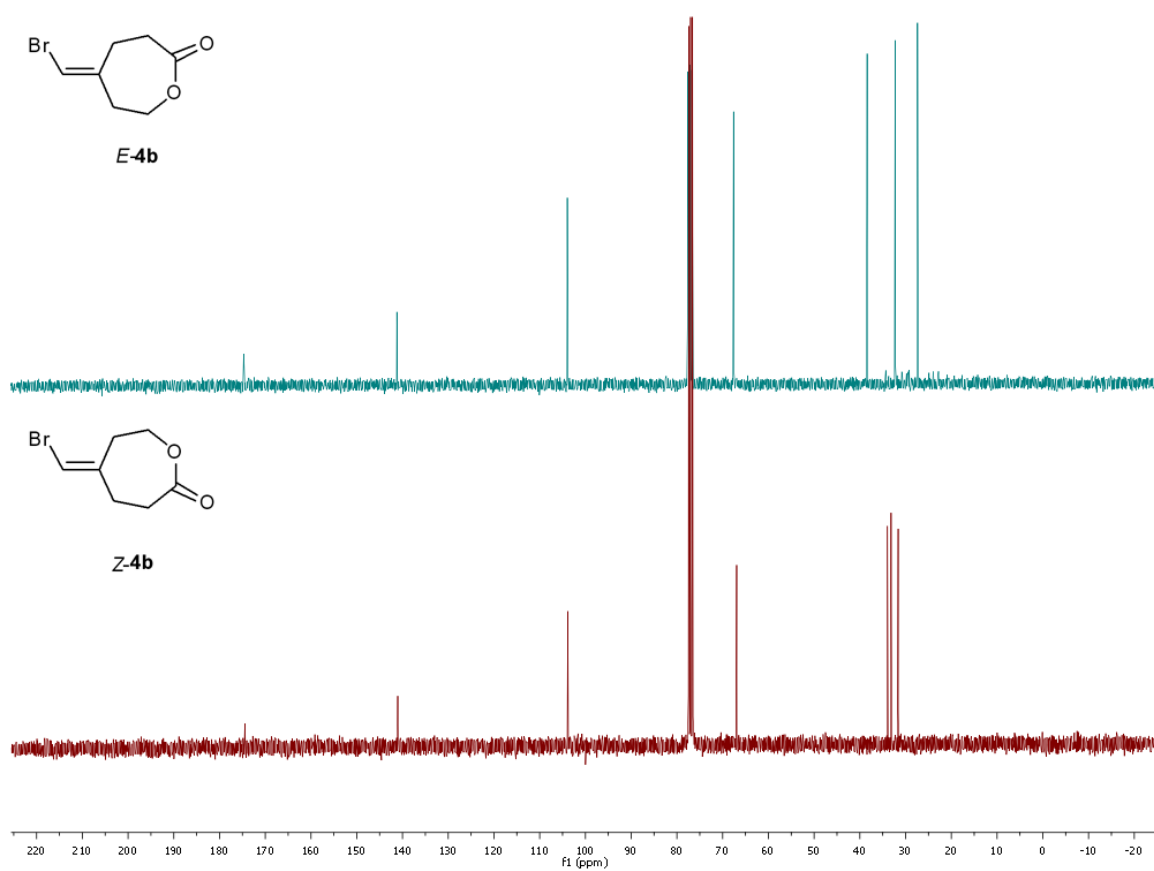
NOESY spectrum of compound *E*-4a (CDCl₃)



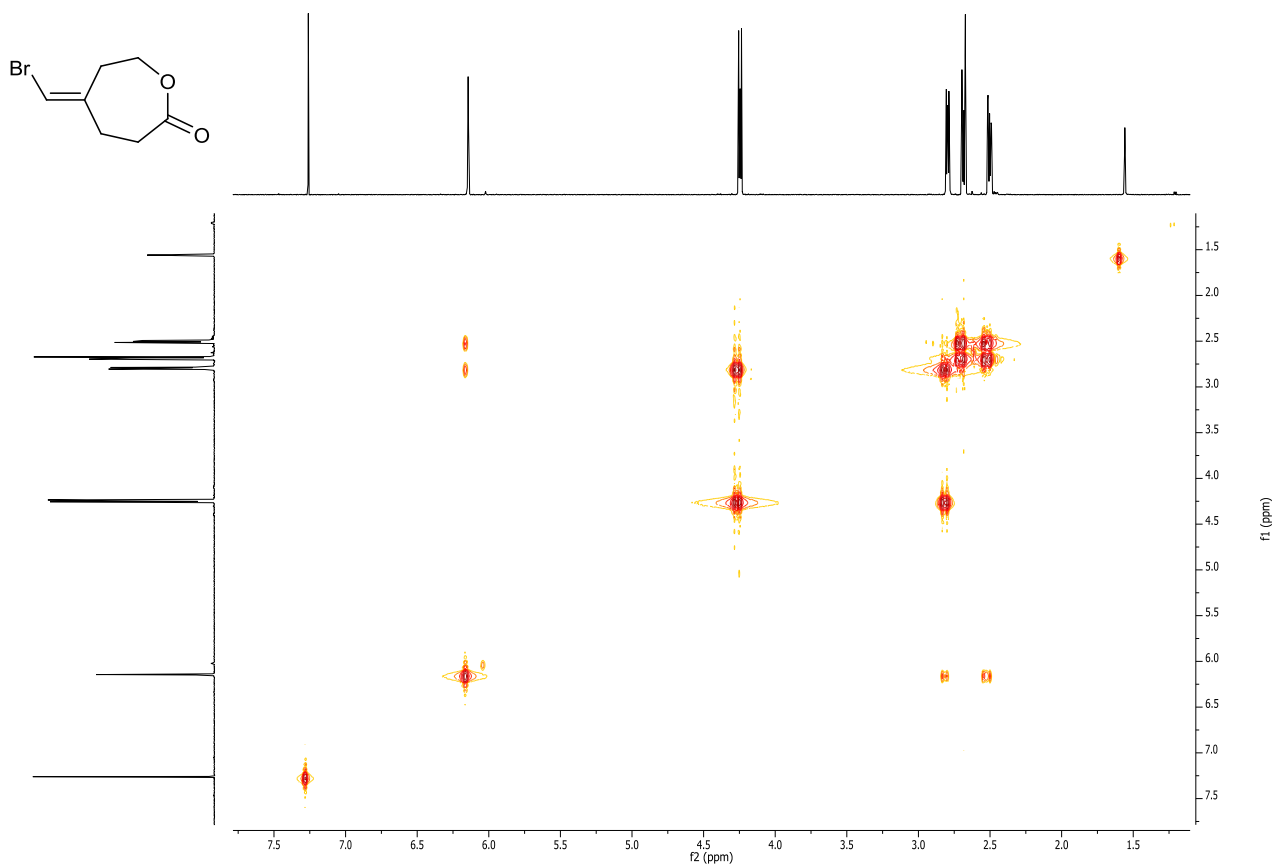
^1H NMR spectra of compounds *E*-4b and *Z*-4b (300 MHz, CDCl_3)



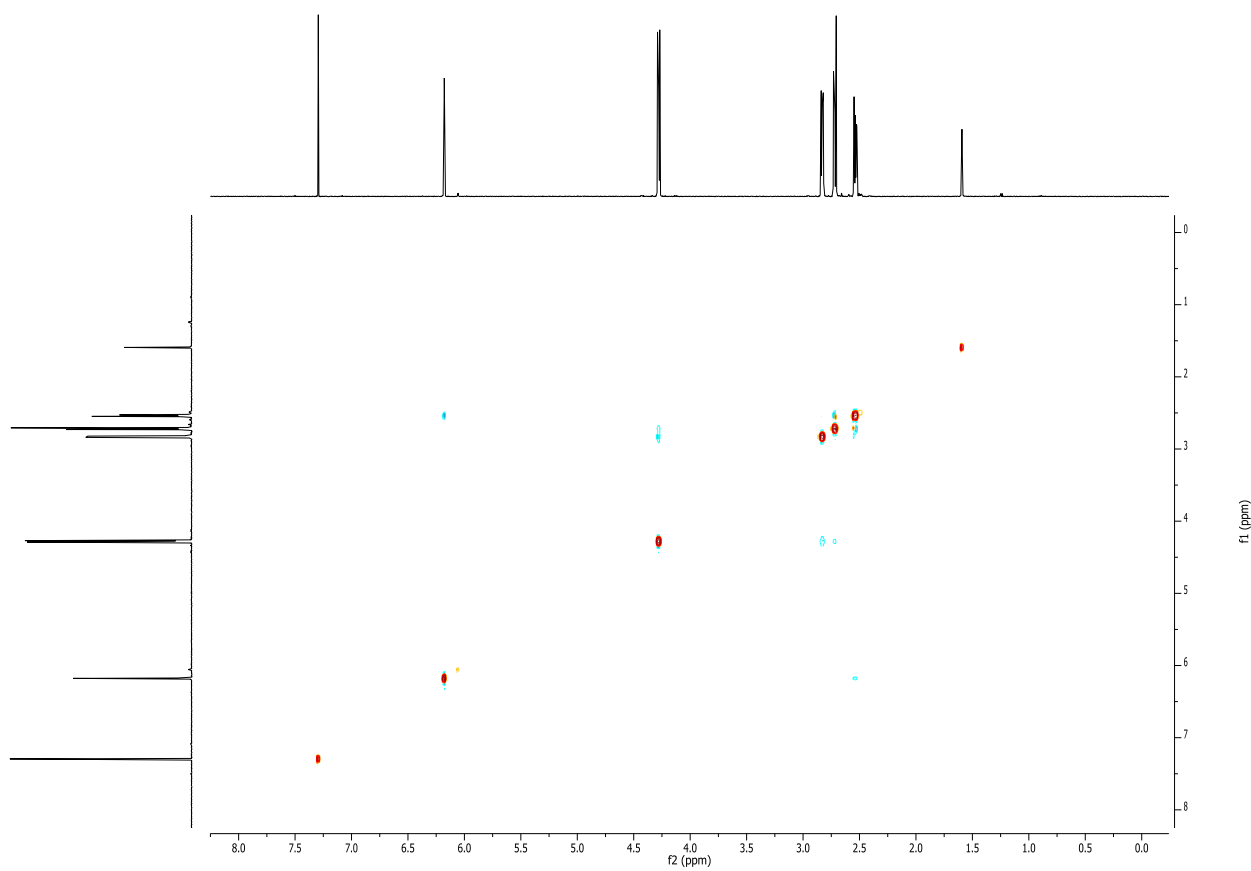
^{13}C NMR spectra of compounds *E*-4b and *Z*-4b (75 MHz, CDCl_3)



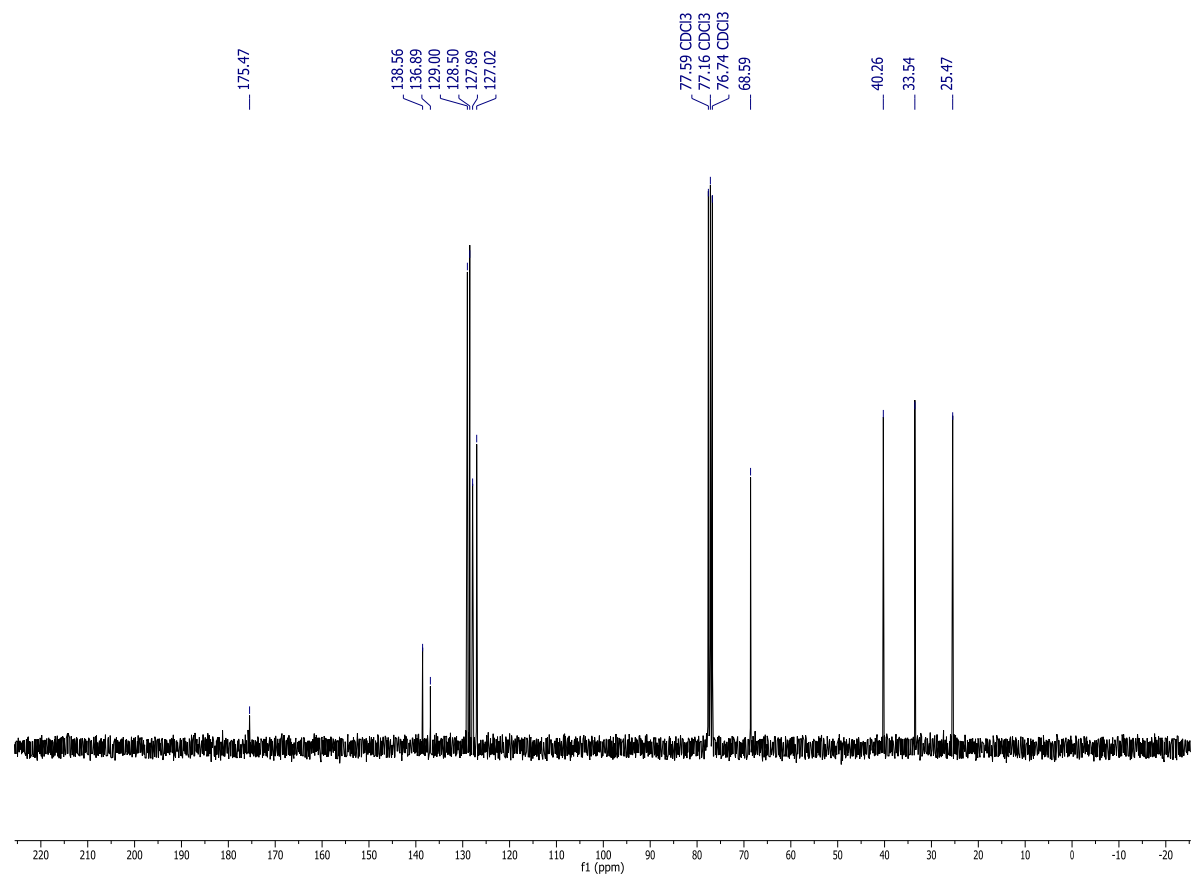
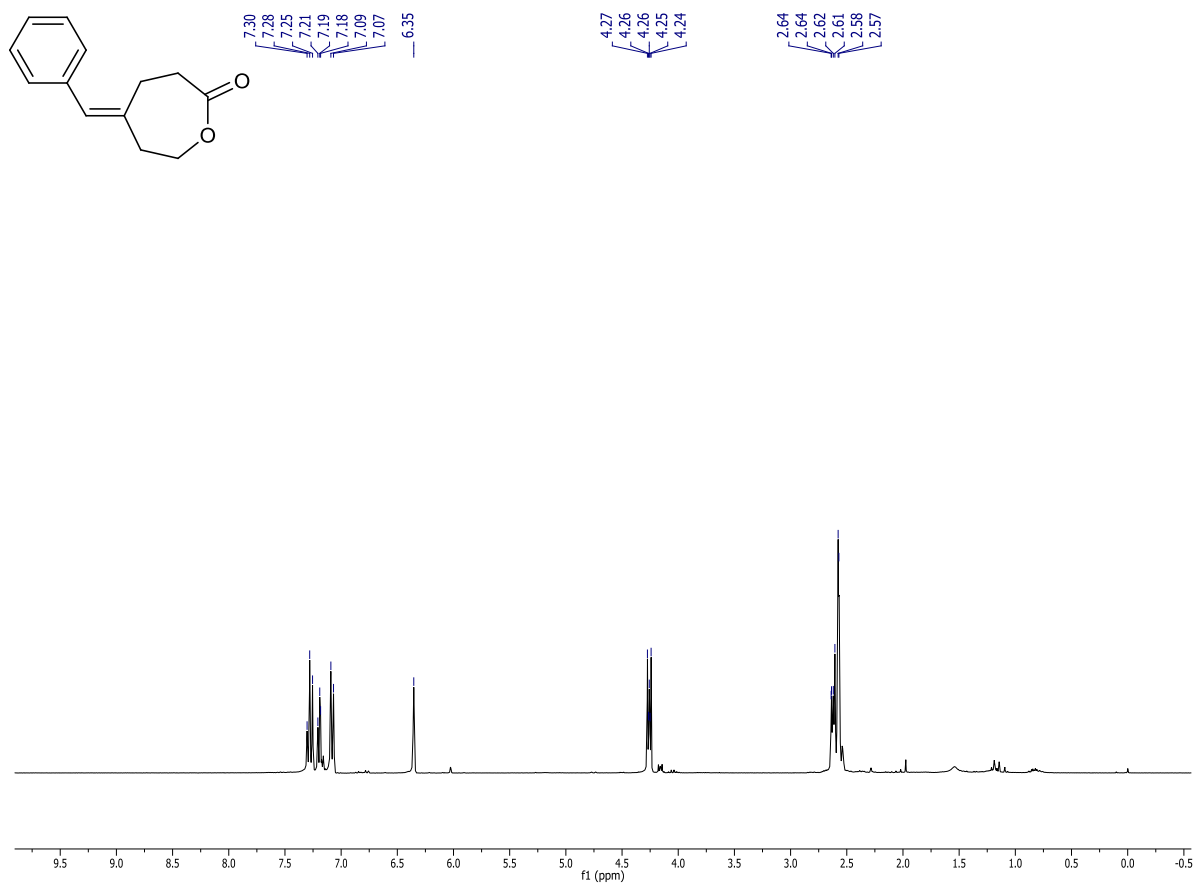
COSY spectrum of compound Z-4b (CDCl₃)



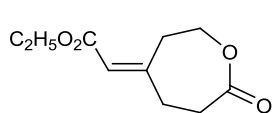
NOESY spectrum of compound Z-4b (CDCl₃)



¹H NMR (300 MHz, CDCl₃) and ¹³C NMR (75 MHz, CDCl₃) spectra of compound E-4c



^1H NMR (300 MHz, CDCl_3) and ^{13}C NMR (75 MHz, CDCl_3) spectra of compound Z-4d



7.26

5.78
5.77
5.77

4.28
4.27
4.27

4.26
4.26
4.26

4.25
4.19
4.16

4.14
4.12

3.33
3.33
3.30

3.30

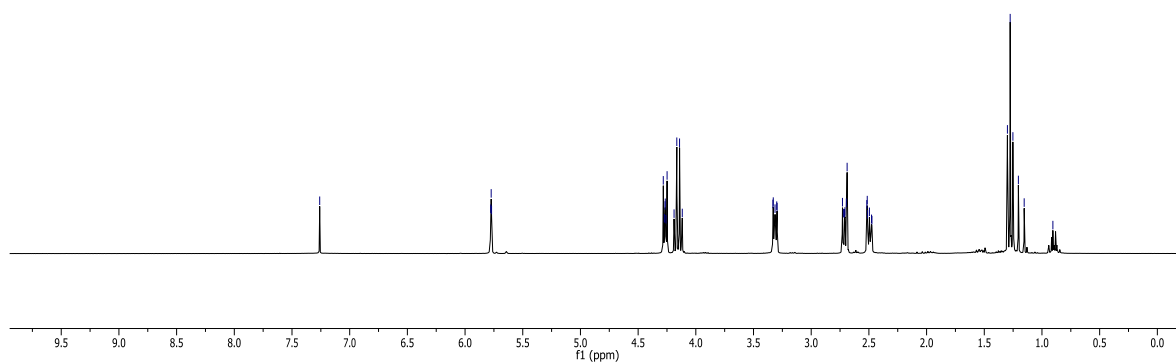
2.73
2.72
2.71

2.70
2.69
2.52

2.51
2.50
2.50

1.28
1.25
1.20

1.15
0.91



174.60

166.11

156.40

118.06

77.58 CDCl_3
77.16 CDCl_3
76.74 CDCl_3

67.34

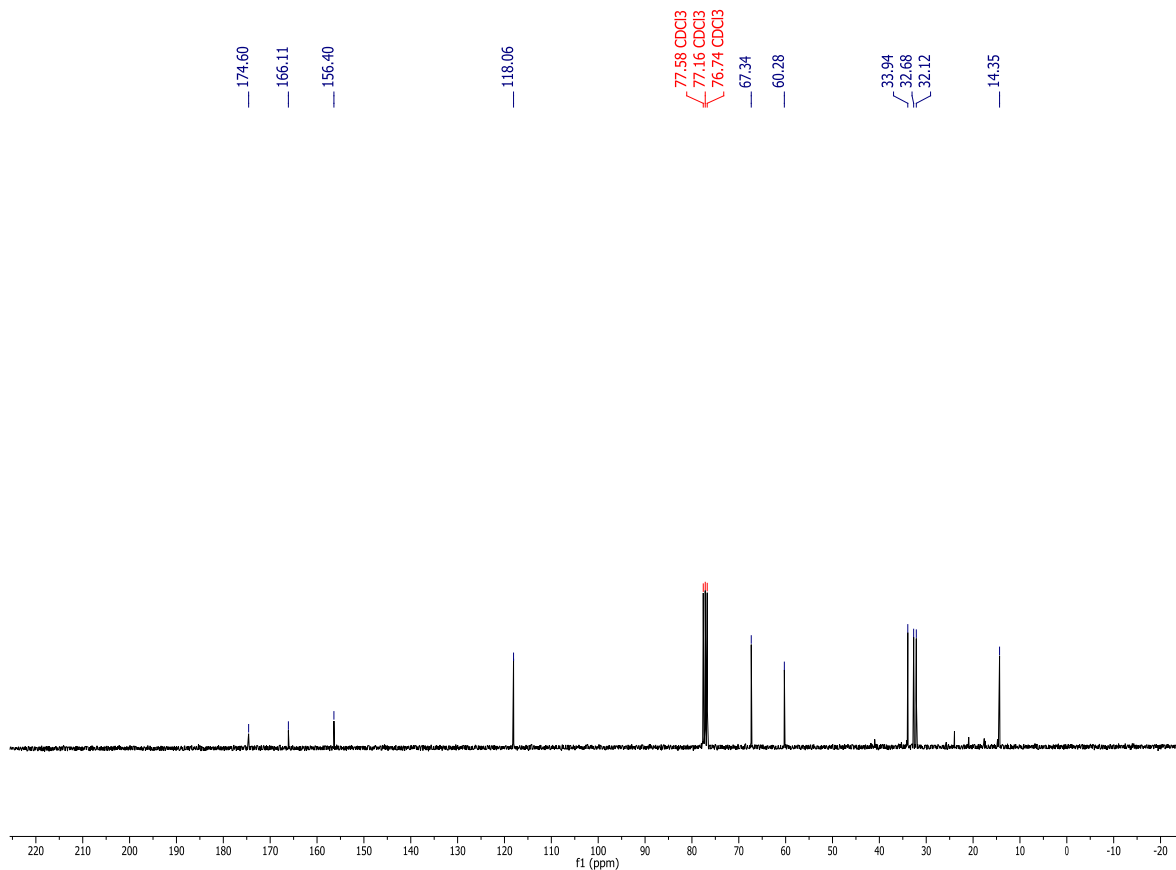
60.28

33.94

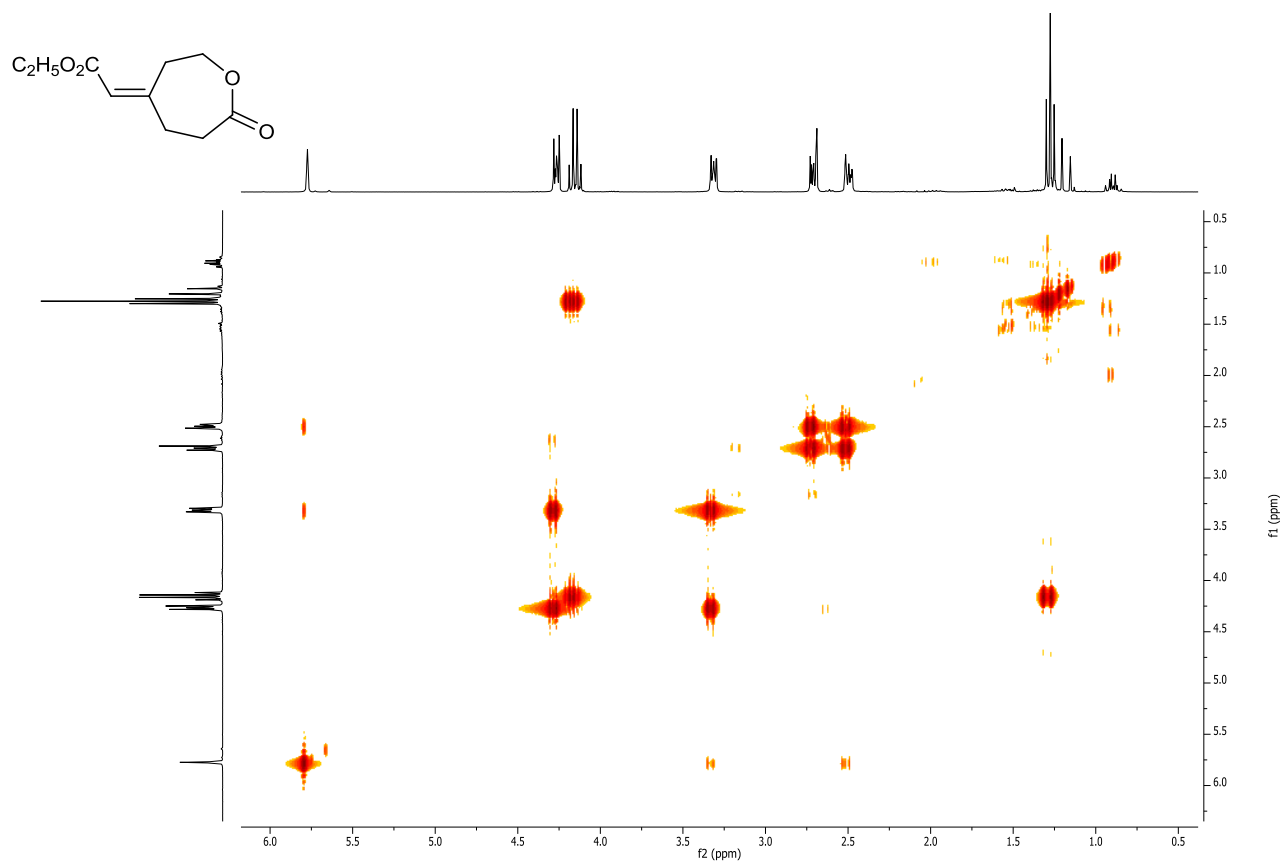
32.68

32.12

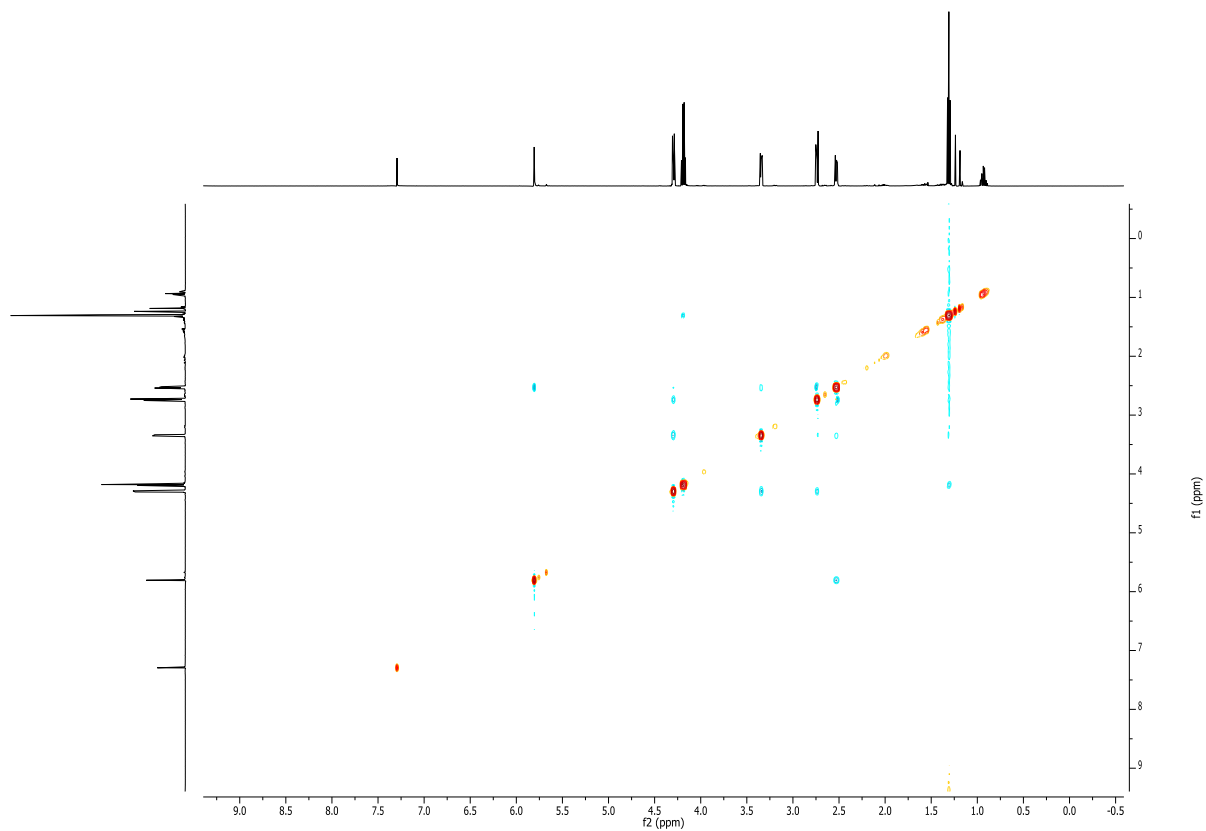
14.35



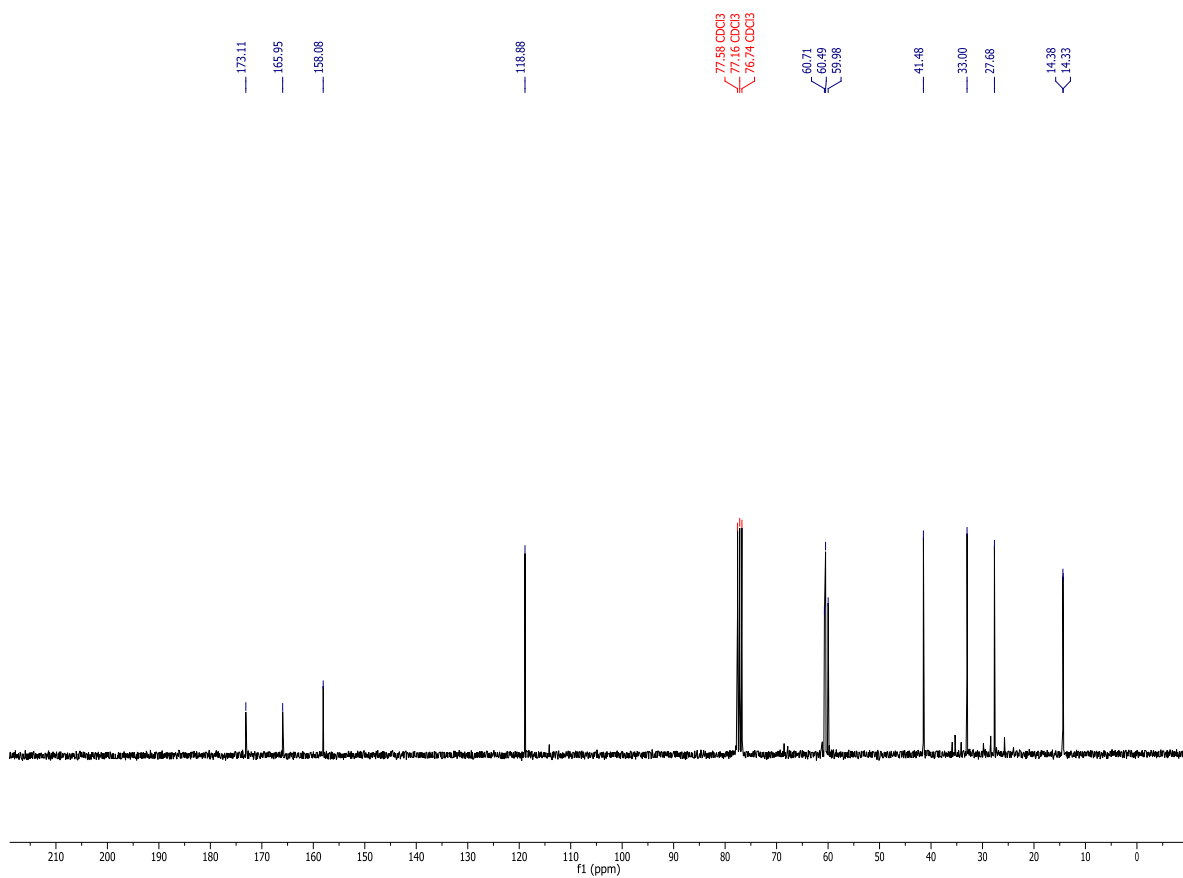
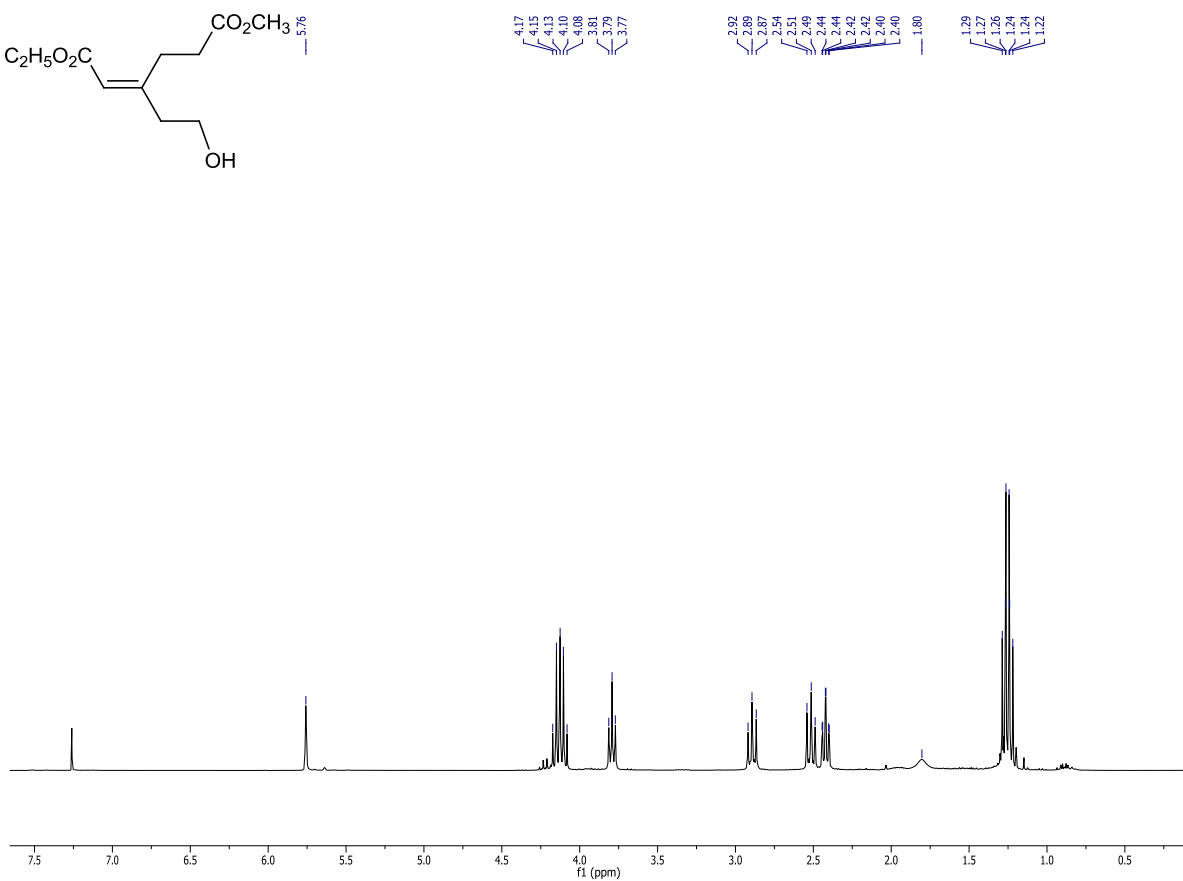
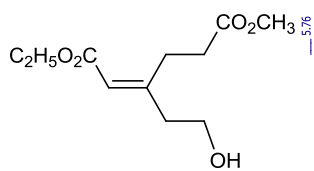
COSY spectrum of compound Z-4d (CDCl₃)



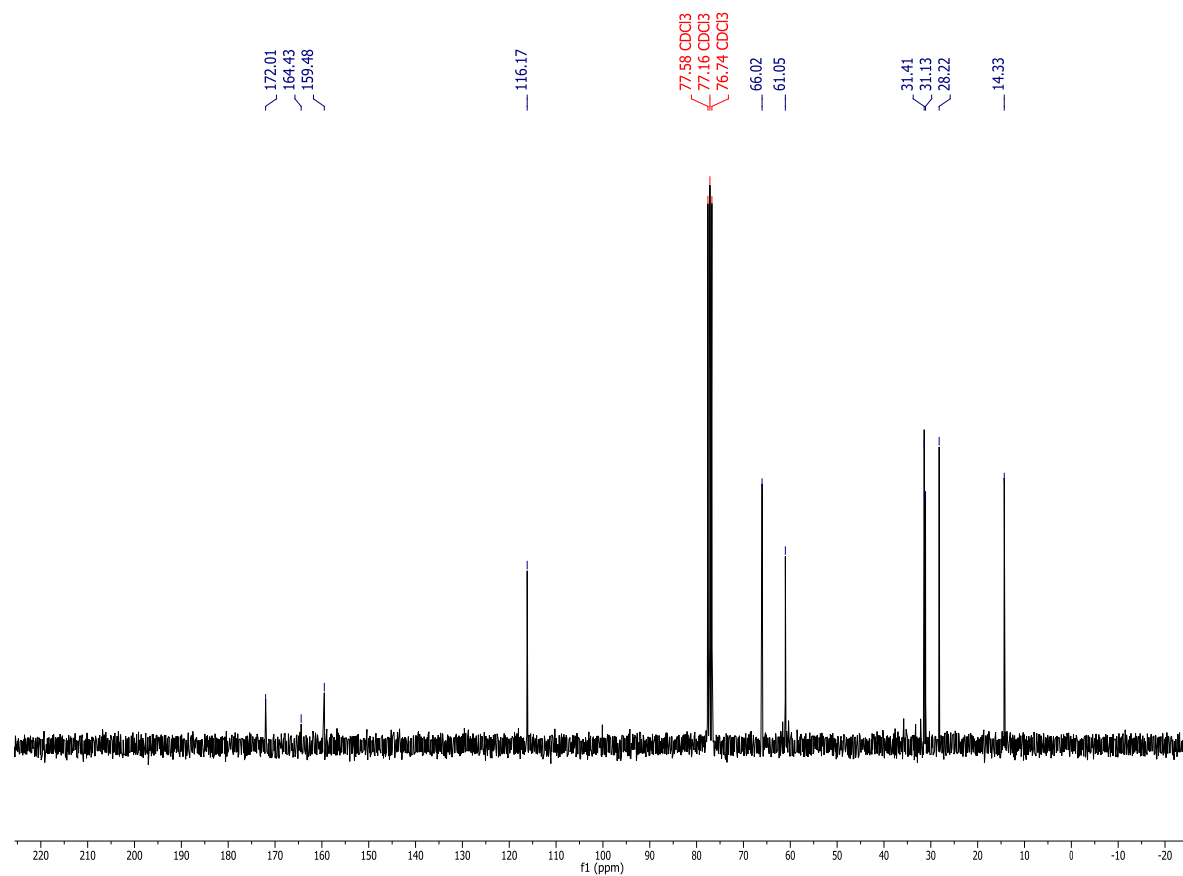
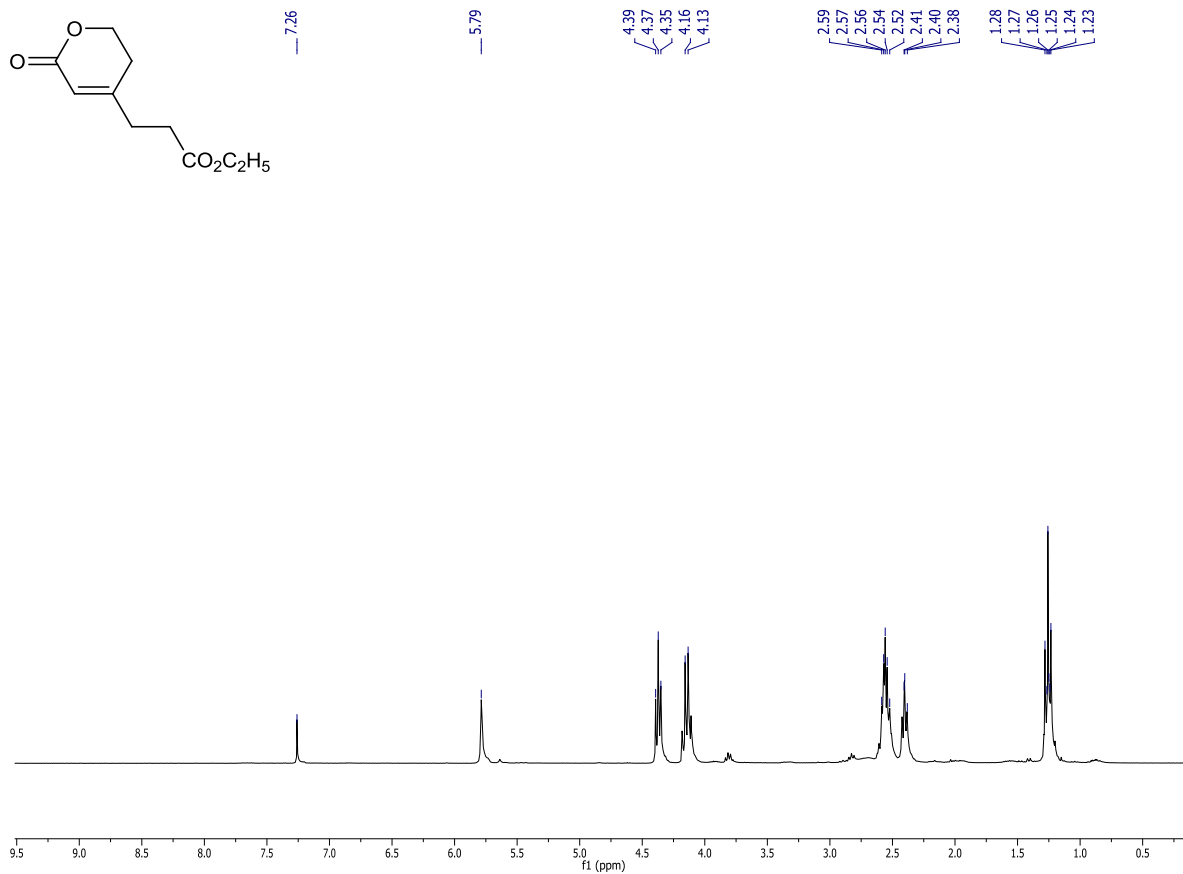
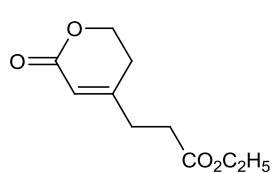
NOESY spectrum of compound Z-4d (CDCl₃)



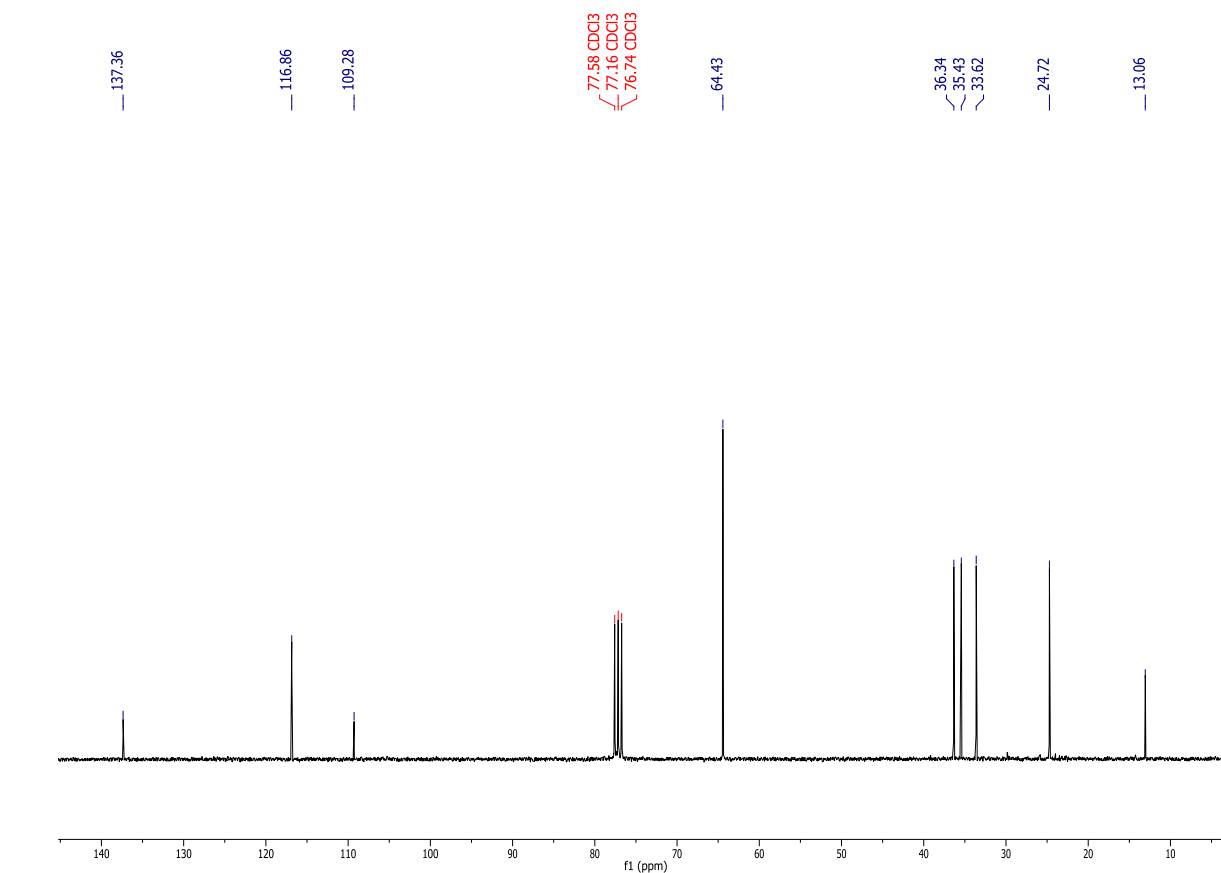
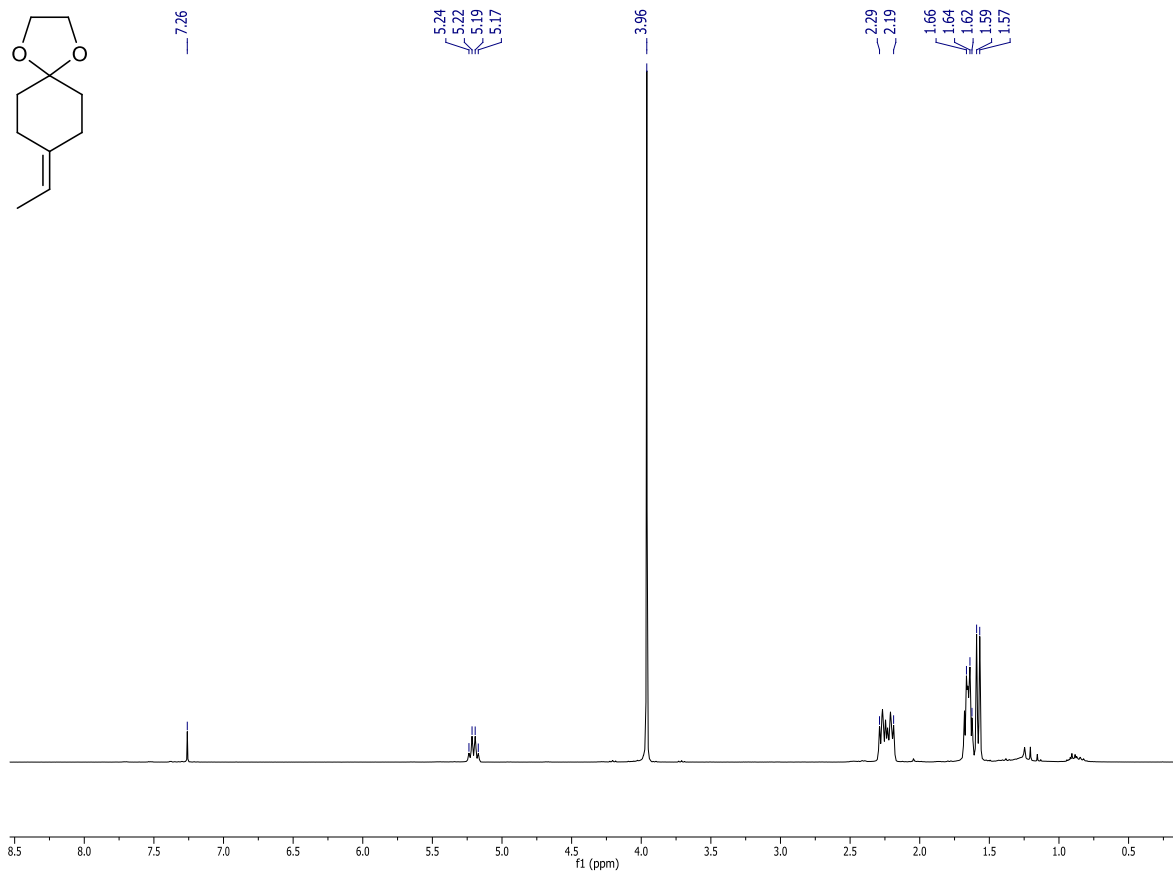
^1H NMR (300 MHz, CDCl_3) and ^{13}C NMR (75 MHz, CDCl_3) spectra of compound E-5



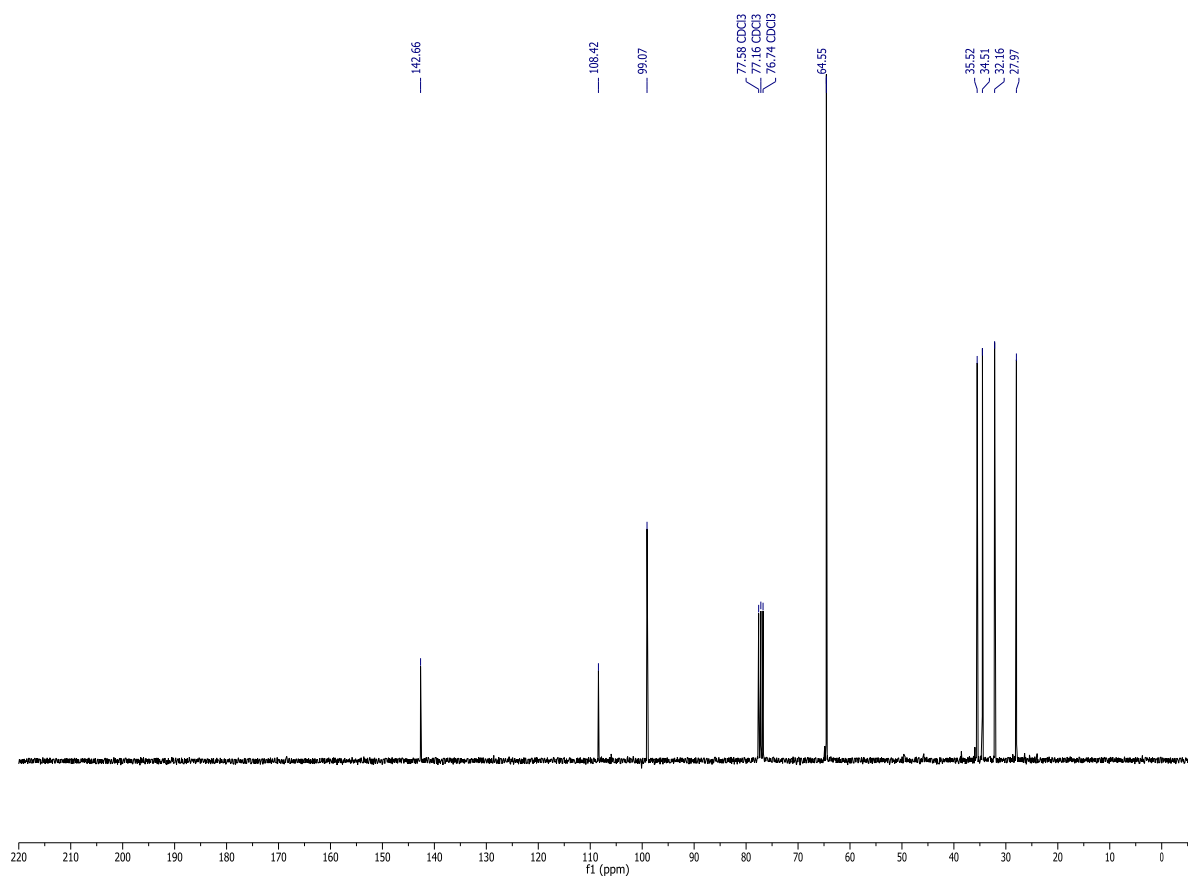
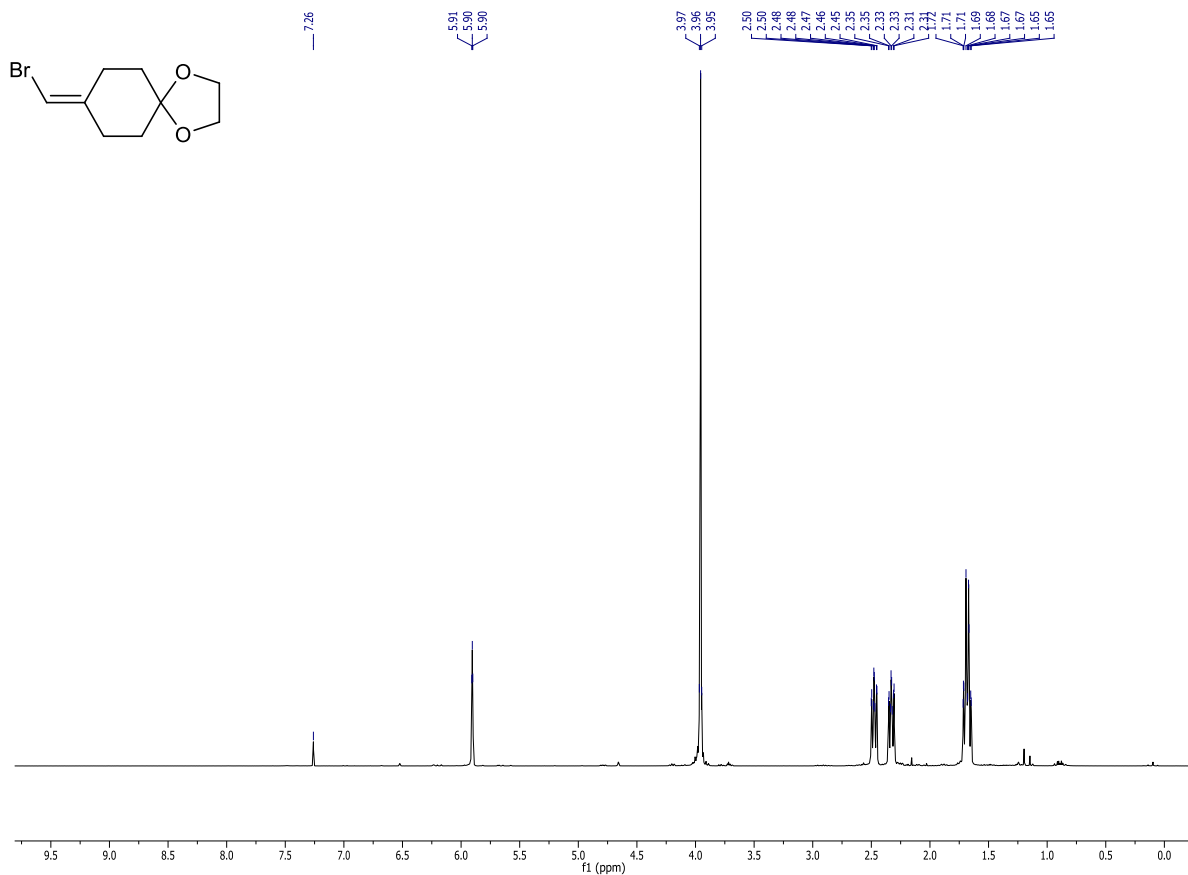
^1H NMR (300 MHz, CDCl_3) and ^{13}C NMR (75 MHz, CDCl_3) spectra of compound 6



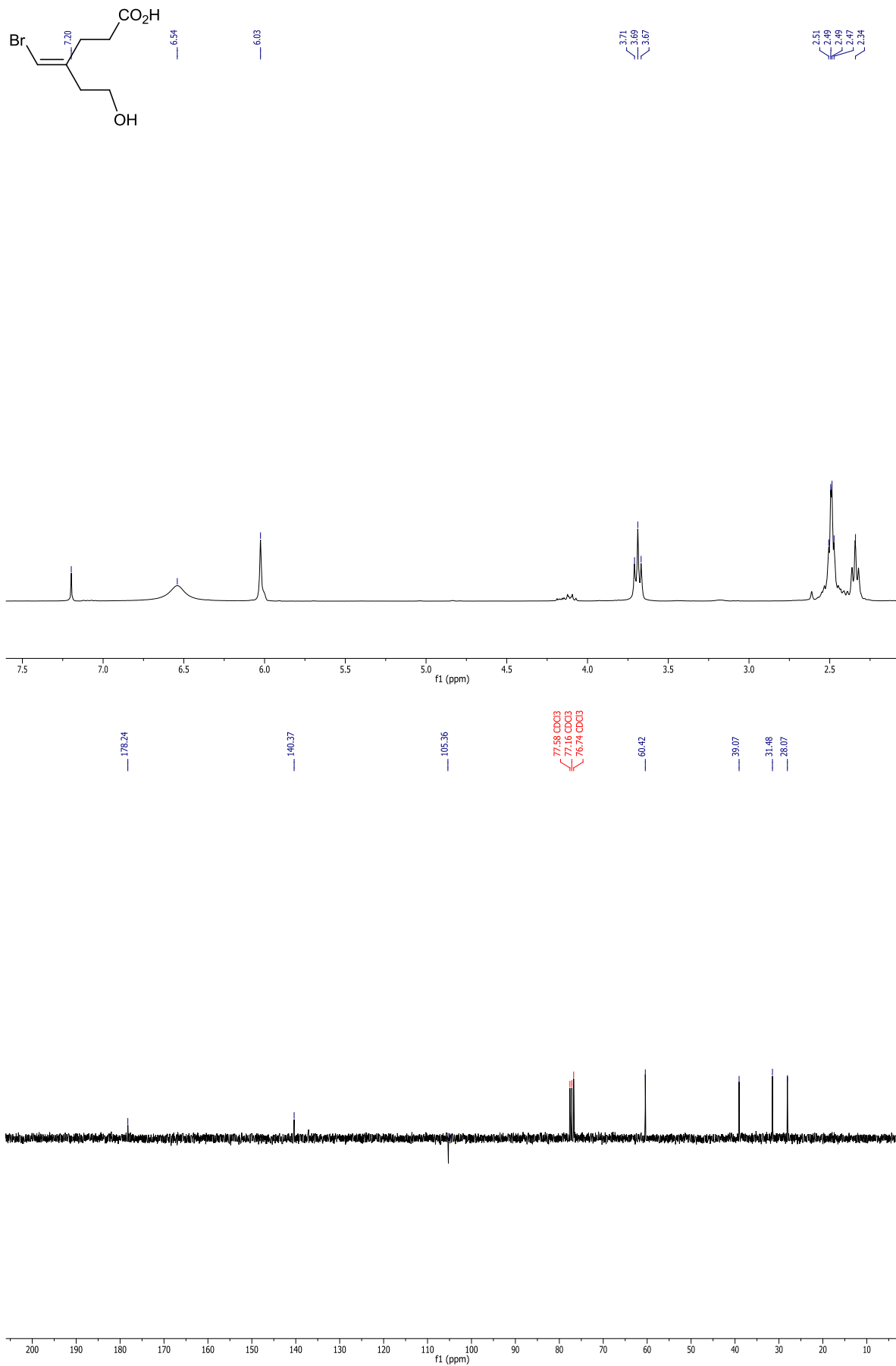
^1H NMR (300 MHz, CDCl_3) and ^{13}C NMR (75 MHz, CDCl_3) spectra of compound S1



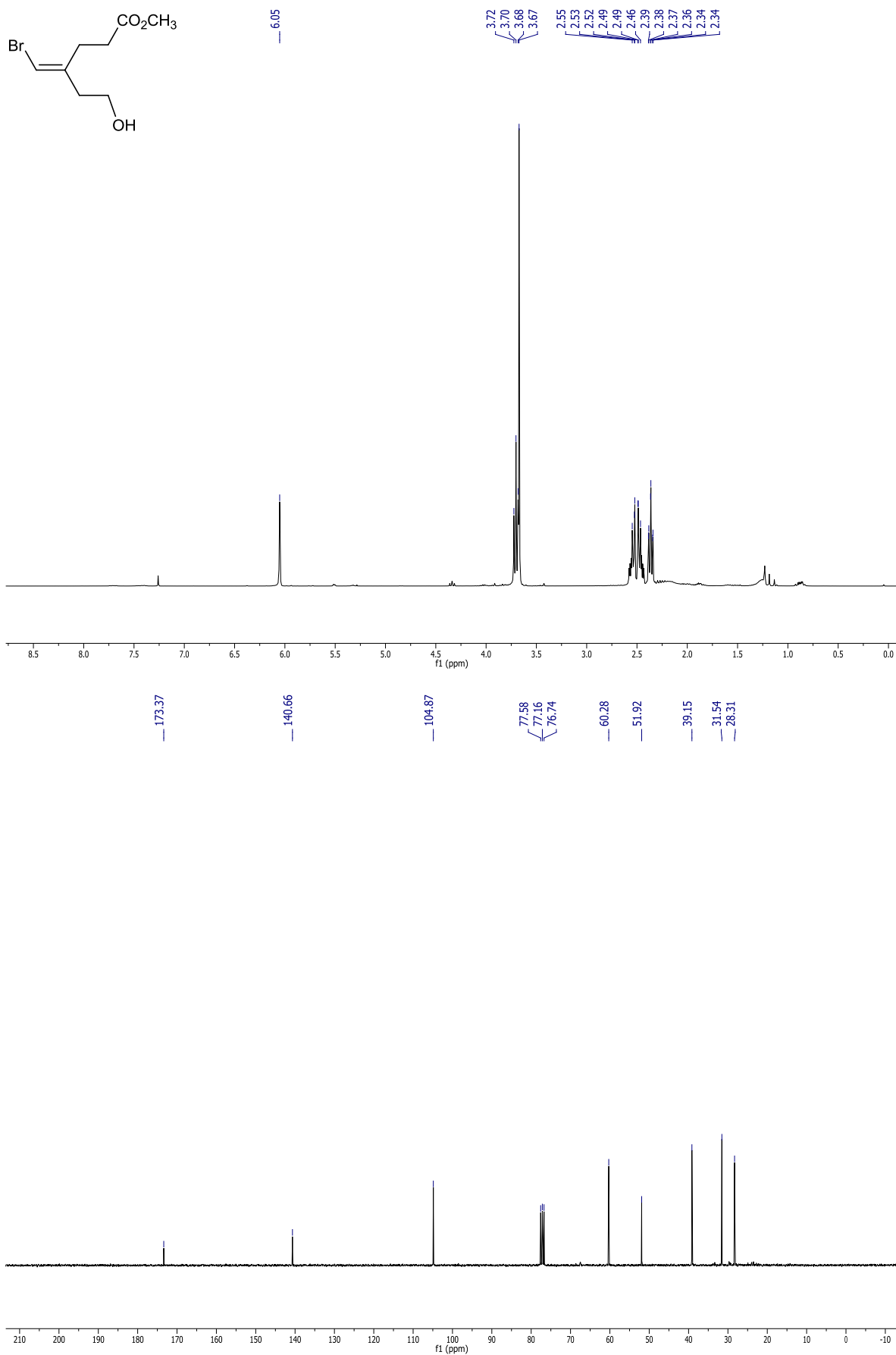
¹H NMR (300 MHz, CDCl₃) and ¹³C NMR (75 MHz, CDCl₃) spectra of compound S2



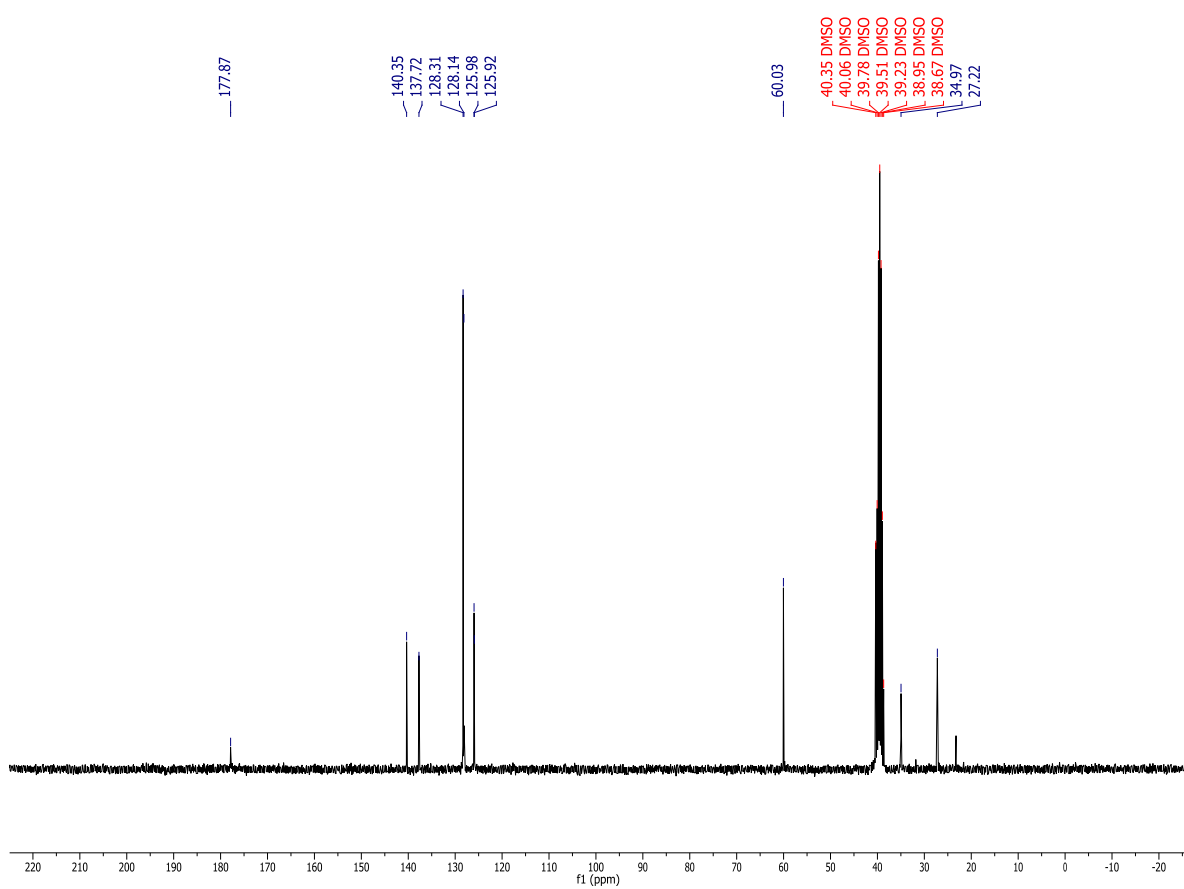
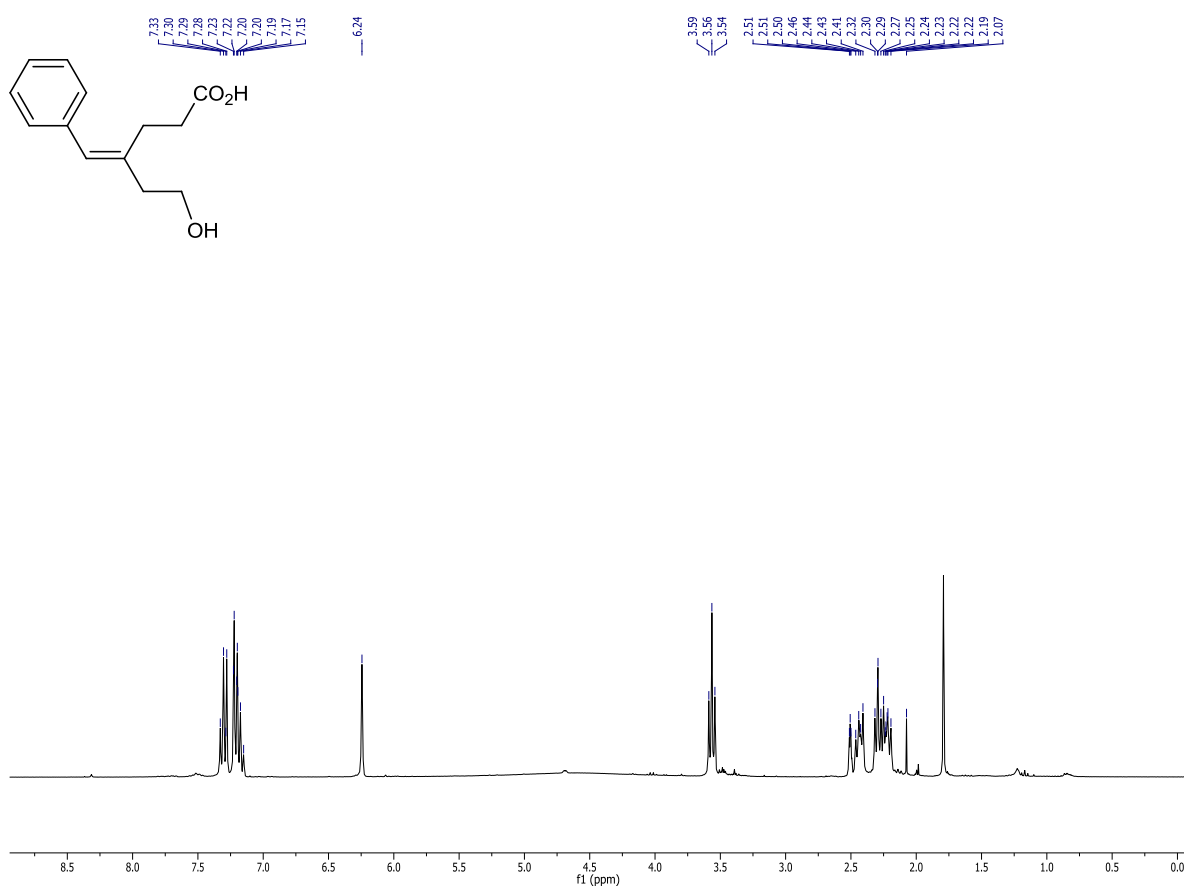
^1H NMR (300 MHz, CDCl_3) and ^{13}C NMR (75 MHz, CDCl_3) spectra of compound S3



^1H NMR (300 MHz, CDCl_3) and ^{13}C NMR (75 MHz, CDCl_3) spectra of compound S4



¹H NMR (300 MHz, DMSO-d₆) and ¹³C NMR (75 MHz, DMSO-d₆) spectra of compound S5



Determination of conversion and diastereoisomeric composition (*cis/trans*)

GC analyses

Compound	Achiral Analysis	
	Conditions	Retention time (min)
<i>E-4a</i> and <i>Z-4a</i>	15 m DB-Wax, inner diameter of 0.25 mm; film thickness of 0.15 μm , pressure: 0.4 bar H_2 ; injector: 230 $^\circ\text{C}$; oven: temperature gradient: 80–260 $^\circ\text{C}$ with 6 $^\circ\text{C}/\text{min}$ from 260 $^\circ\text{C}$ 5 min isothermic, FID detector: 350 $^\circ\text{C}$.	14.51 <i>cis</i> 14.71 <i>trans</i>
<i>E-4b</i> and <i>Z-4b</i>	15 m DB-Wax, inner diameter of 0.25 mm; film thickness of 0.15 μm , pressure: 0.4 bar H_2 ; injector: 230 $^\circ\text{C}$; oven: temperature gradient: 80–260 $^\circ\text{C}$ with 6 $^\circ\text{C}/\text{min}$ from 260 $^\circ\text{C}$ 5 min isothermic, FID detector: 350 $^\circ\text{C}$.	18.22 <i>cis</i> 18.55 <i>trans</i>
<i>E-4c</i>	15 m DB-Wax, inner diameter of 0.25 mm; film thickness of 0.15 μm , pressure: 0.4 bar H_2 ; injector: 230 $^\circ\text{C}$; oven: temperature gradient: 80–260 $^\circ\text{C}$ with 6 $^\circ\text{C}/\text{min}$ from 260 $^\circ\text{C}$ 5 min isothermic, FID detector: 350 $^\circ\text{C}$.	21.54 <i>trans</i>
<i>E-4d</i> and <i>Z-4d</i>	15 m DB-Wax, inner diameter of 0.25 mm; film thickness of 0.15 μm , pressure: 0.4 bar H_2 ; injector: 230 $^\circ\text{C}$; oven: temperature gradient: 80–260 $^\circ\text{C}$ with 6 $^\circ\text{C}/\text{min}$ from 260 $^\circ\text{C}$ 5 min isothermic, FID detector: 350 $^\circ\text{C}$.	21.12 <i>cis</i> 21.63 <i>trans</i>

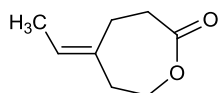
Preparative HPLC for compound 4b

In the case of compound **4b** preparative HPLC was used to separate the *cis* and *trans* diastereoisomers.

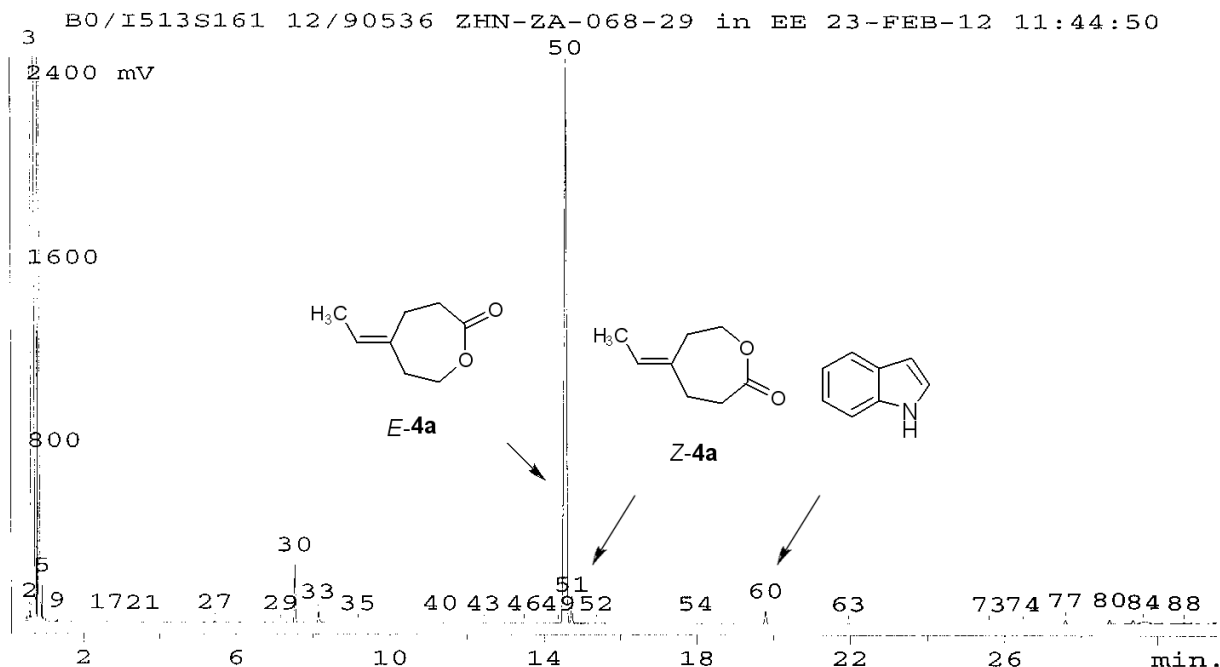
Compound	Analytical separation		Preparative separation	
	Conditions	Retention time (min)	Conditions	Retention time (min)
4b	100 mm Interchim Strategy 2.2 Si, 4.6 mm i. D. <i>n</i> -Heptane/ <i>iso</i> -propanol=90:10; flow: 1.0 mL/min, 7.6 MPa, 308 K; UV, 210 nm.	3.54 (<i>cis</i>), 4.41 (<i>trans</i>)	Stationary phase: LiChrospher Si100, 10 μm , 20 mm i. D.; column: 250 x 20 mm BIAX-Säule, 95/17; iso-Hexane/ iso-Propanol=95:5; flow: 10.0 mL/min, 0.2 MPa, 308 K; Detection UV, 210 nm.	15.6 (<i>cis</i>), 20.3 (<i>trans</i>)

GC Chromatograms

Preparation of (*E*)-4-ethylidene- ϵ -caprolactone (*E*-4a) resulting from biocatalytic Baeyer-Villiger reaction of 3a with WT CHMO



Achiral chromatogram



***** R513S161.DAT ***** 23-FEB-12 13:41:51

Sample : 12/90536 measured: 23-FEB-12 11:44:50
 Cust.ID: ZHN-ZA-068-29 processed: 23-FEB-12 13:41:09
 S.code : in EE by: CHROM3
 with:

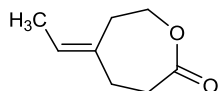
achirale Uebersichtsanalyse, Auswertung ohne Loesemittelbereich sup bis 3.5min

No.	min.	area-%
30	7.55	4.42
33	8.16	1.08
50	14.60	87.9
51	14.73	1.67
60	19.80	1.32
77	27.59	0.44
80	28.75	0.50
83	29.36	0.45
84	29.64	1.19

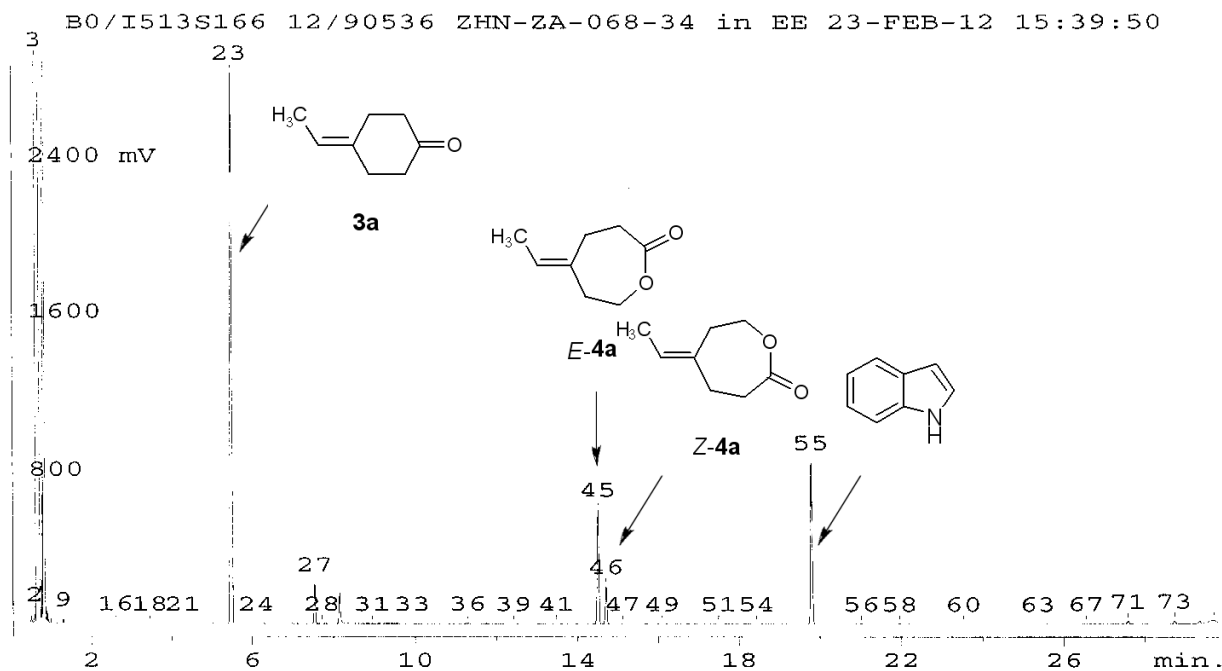
%- threshold: 0.10 %
 60 peaks out of 69 (total area percentage = 1.06 %) are below threshold.
 34 peaks had been suppressed.

Instrument : HP6890 / MPS2L , 513
 Column : 15m DB-Wax 0.25/0.15df G/492
 Detector : FID
 Temperature : 230/60 6/min 260 5min iso/350
 Gas : 0.4 bar H2
 Sample size : 1 uL
 Recorder : 1mV

Preparation of (Z)-4-ethylidene-ε-caprolactone (Z-4a) resulting from biocatalytic Baeyer-Villiger reaction of 3a with Mutant CHMO



Achiral chromatogram



***** R513S166.DAT ***** 24-FEB-12 07:29:33

Sample : 12/90536 measured: 23-FEB-12 15:39:50
Cust.ID: ZHN-ZA-068-34 processed: 24-FEB-12 07:29:16
S.code : in EE by: CHROM3
with:

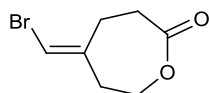
achirale Uebersichtsanalyse, Auswertung ohne Loesemittelbereich sup bis 3.5min

No.	min.	area-%
23	5.51	58.7
27	7.54	3.24
30	8.16	3.00
45	14.51	12.2
46	14.71	3.77
55	19.79	17.2
71	27.59	0.33
73	28.75	0.37
77	29.37	0.37

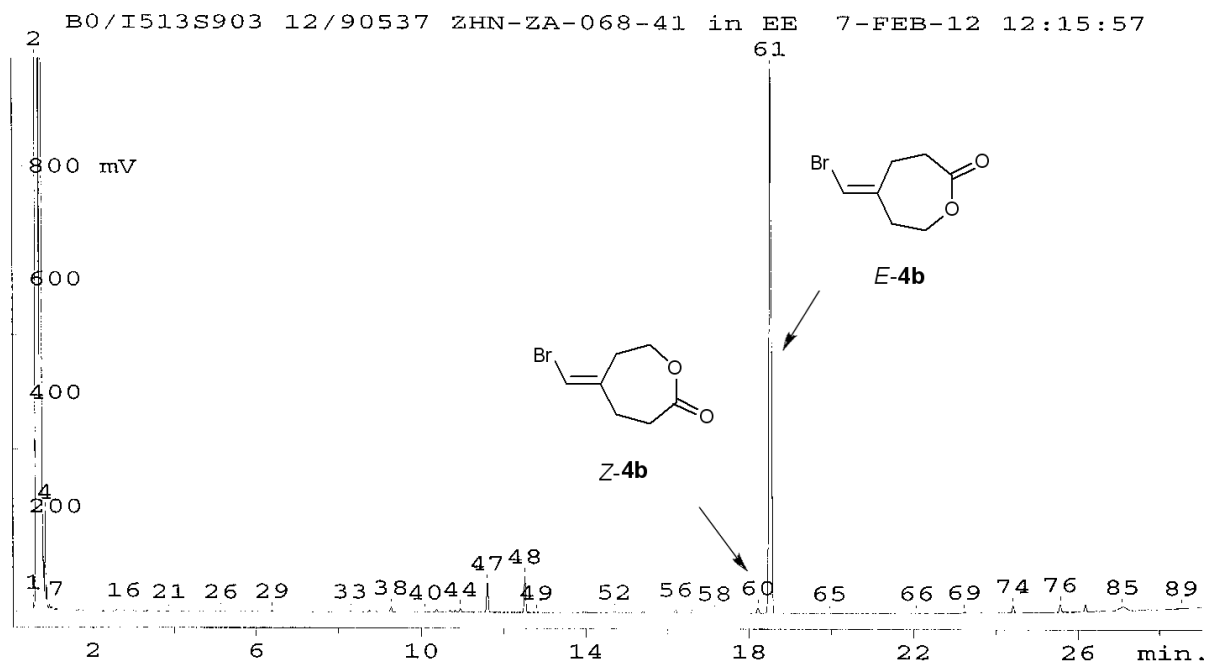
%- threshold: 0.10 %
50 peaks out of 59 (total area percentage = 0.79 %) are below threshold.
37 peaks had been suppressed.

Instrument : HP6890 / MPS2L , 513
Column : 15m DB-Wax 0.25/0.15df G/492
Detector : FID
Temperature : 230/80 6/min 260 5min iso/350
Gas : 0.4 bar H2
Sample size : 1 uL
Recorder : 1mV

Preparation of (E)-4-bromomethylene-ε-caprolactone (E-4b) resulting from biocatalytic Baeyer-Villiger reaction of 3b with WT CHMO



Achiral chromatogram



***** R513S903.DAT ***** 7-FEB-12 15:22:12

Sample : 12/90537 measured: 7-FEB-12 12:15:57
Cust.ID: ZHN-ZA-068-41 processed: 7-FEB-12 15:21:34
S.code : in EE by: CHROM3
with:

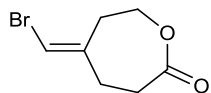
achirale Uebersichtsanalyse, Auswertung ohne Loesemittelbereich sup bis 3min

No.	min.	area-%
38	9.27	0.50
41	10.37	0.31
44	10.95	0.37
47	11.60	3.16
48	12.52	3.76
52	14.70	0.23
56	16.20	0.45
57	16.62	0.45
60	18.22	0.71
61	18.55	81.3
74	24.41	0.88
76	25.57	0.98
81	26.18	0.83
85	27.09	2.22

%- threshold: 0.20 %
56 peaks out of 70 (total area percentage = 3.88 %) are below threshold.
28 peaks had been suppressed.

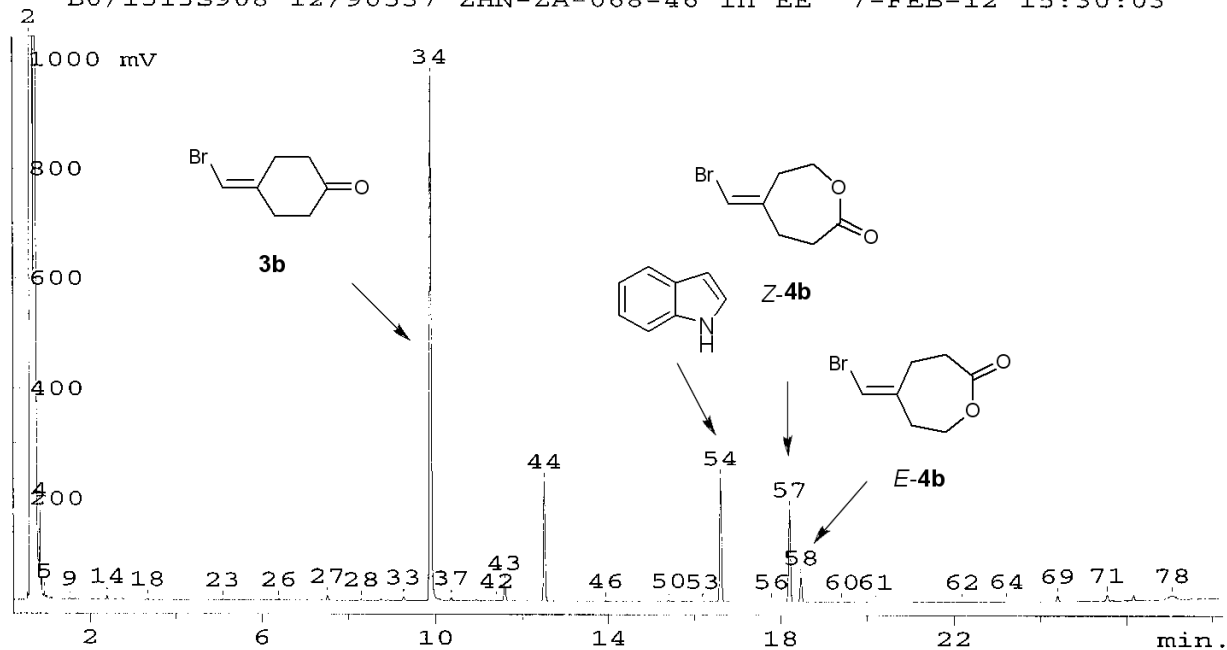
Instrument : HP6890 / MPS2L , 513
Column : 15m DB-Wax 0.25/0.15df G/492
Detector : FID
Temperature : 230/80 6/min 260 5min iso/350
Gas : 0.4 bar H2
Sample size : 1 uL
Recorder : 1mV

Preparation of (Z)-4-bromomethylene- ϵ -caprolactone (Z-4b) resulting from biocatalytic Baeyer-Villiger reaction of 3b with Mutant CHMO



Achiral chromatogram

B0/I513S908 12/90537 ZHN-ZA-068-46 in EE 7-FEB-12 15:30:03



***** R513S908.DAT ***** 8-FEB-12 07:43:21

Sample : 12/90537 measured: 7-FEB-12 15:30:03
 Cust.ID: ZHN-ZA-068-46 processed: 8-FEB-12 07:42:39
 S.code : in EE by: CHROM3
 with:

achirale Uebersichtsanalyse, Auswertung ohne Loesemittelbereich sup bis 3min

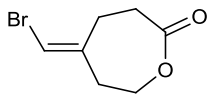
No.	min.	area-%
27	7.52	0.38
33	9.27	0.35
34	9.90	54.1
35	10.08	0.27
37	10.36	0.26
43	11.60	1.76
44	12.51	10.9
54	16.61	12.9
57	18.21	10.2
58	18.47	2.55
69	24.40	0.61
71	25.55	0.69
75	26.17	0.58
78	27.07	2.02

%- threshold: 0.15 %
 50 peaks out of 64 (total area percentage = 2.47 %) are below threshold.
 26 peaks had been suppressed.

Instrument : HP6890 / MPS2L , 513
 Column : 15m DB-Wax 0.25/0.15df G/492
 Detector : FID
 Temperature : 230/80 6/min 260 5min iso/350
 Gas : 0.4 bar H2
 Sample size : 1 uL
 Recorder : 1mV

HPLC Chromatograms

Mixture of (*E*)-4-bromomethylene- ϵ -caprolactone (*E*-4b) and (*Z*)-4-bromomethylene- ϵ -caprolactone (*Z*-4b) (87:13 *trans/cis*)



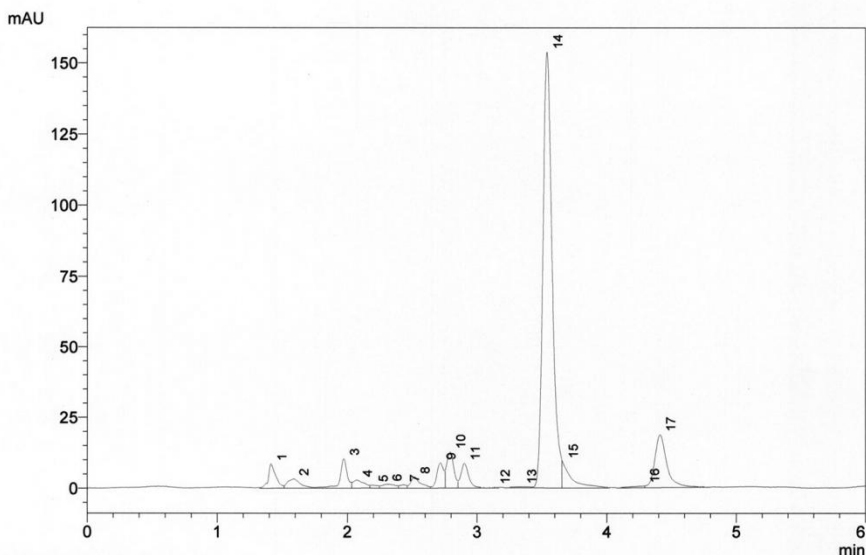
Sample resulted from the first column chromatography of the biocatalytic Baeyer-Villiger reaction product of **1b** with Mutant CHMO.

Achiral chromatogram

Gerät : LC-2010-1

Operator :
Sample Name : ROI-RA-253-03
Vial # : 11
Injection Volume : 1 μ L
Data File Name : ROI-RA-253-03-06.lcd
Method File Name : Roiban.lcm
Data Acquired: 16.03.2012 09:55:41

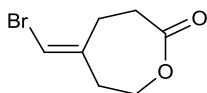
1 μ L ROI-RA-253-03 präp. Lösung 1:100
100 mm Interchim Strategy 2.2 Si, 4.6 mm i. D. ,
n-Heptan/2-Propanol = 90:10
1.0 mL/min, 7.6 MPa, 308 K
210 nm



1 Det.A Ch1/210nm

Peak #	Ret. Time	Area %	Name
1	1.41	2.79	
2	1.58	1.74	
3	1.97	3.14	
4	2.07	1.32	
5	2.19	0.29	
6	2.30	0.70	
7	2.43	0.29	
8	2.52	1.52	
9	2.72	2.67	
10	2.79	4.06	
11	2.90	2.93	
12	3.13	0.01	
13	3.34	0.11	
14	3.54	64.60	cis
15	3.66	3.60	
16	4.29	0.25	
17	4.41	9.98	trans
Total		100.00	

Separated (*E*)-4-bromomethylene- ϵ -caprolactone (*E*-4b)



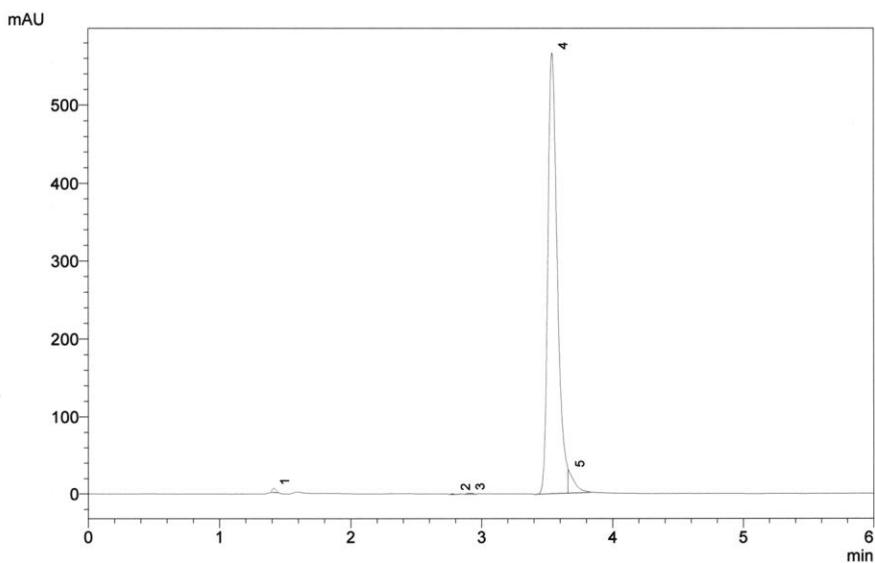
Achiral chromatogram

Gerät : LC-2010-1

Operator :
Sample Name : ROI-RA-253-20
Vial # : 12
Injection Volume : 1 μ L
Data File Name : ROI-RA-253-20-04.lcd
Method File Name : Roiban.lcm

Data Acquired: 16.03.2012 10:02:10

2 μ L ROI-RA-253-20 (1.03 mg in 0.5 ml 2-Propanol)
nach der Aufarbeitung
100 mm Interchim Strategy 2.2 Si, 4.6 mm i. D.,
n-Heptan/2-Propanol = 90:10
1.0 mL/min, 7.6 MPa, 308 K
210 nm

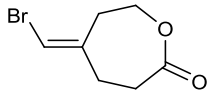


1 Det.A Ch1/210nm

Detector A Ch1 210nm

Peak #	Ret. Time	Area %	Name
1	1.41	0.31	
2	2.79	0.02	
3	2.90	0.07	
4	3.54	96.43	cis
5	3.67	3.16	
Total		100.00	

Separated (Z)-4-bromomethylene-ε-caprolactone (Z-4b)



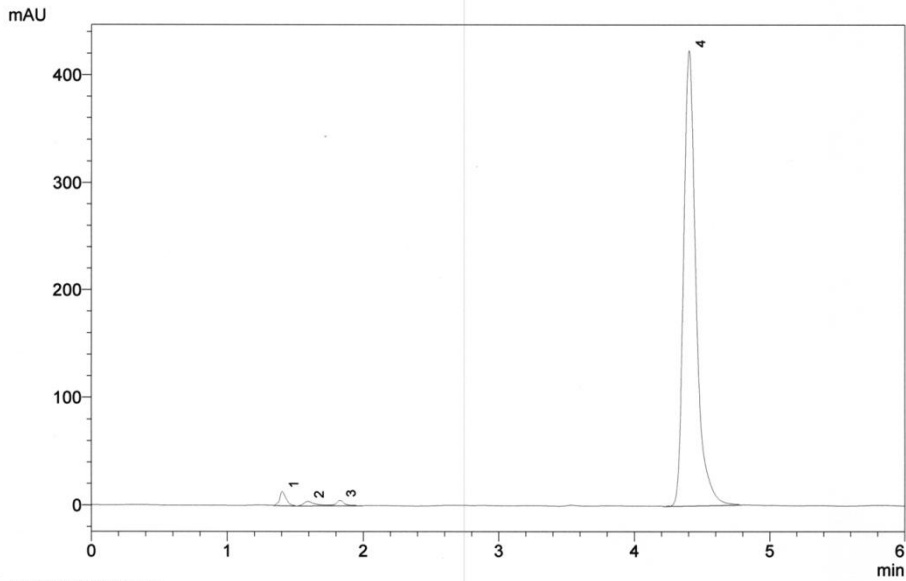
Achiral chromatogram

Gerät : LC-2010-1

Operator :
Sample Name : ROI-RA-253-40
Vial # : 14
Injection Volume : 2 µL
Data File Name : ROI-RA-253-40-04.lcd
Method File Name : Roiban.lcm

Data Acquired: 16.03.2012 10:15:05

2 µL ROI-RA-253-40 (0.53 mg in 0.5 ml 2-Propanol)
nach der Aufarbeitung
100 mm Interchim Strategy 2.2 Si, 4.6 mm i. D. ,
n-Heptan/2-Propanol = 90:10
1.0 mL/min, 7.6 MPa, 308 K
210 nm



1 Det.A Ch1/210nm

Detector A Ch1 210nm

Peak #	Ret. Time	Area %	Name
1	1.40	1.48	
2	1.59	0.76	
3	1.83	0.67	
4	4.40	97.09	trans
Total		100.00	

X-ray data

Single crystal X-ray structure of compound *E-4b*

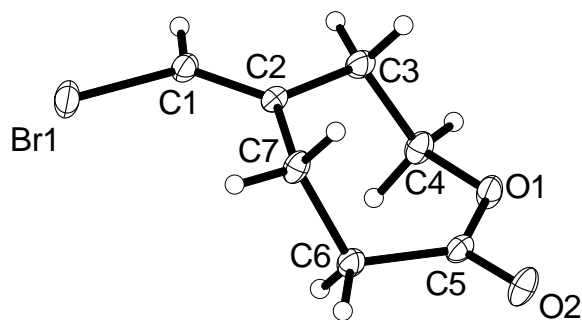


Figure S3 | The molecular structure of *E-4b*. Atomic displacement ellipsoids are shown at the 50% probability level

Crystal Data for *E-4b*: [C₇H₉BrO₂], $M_r = 205.05 \text{ g} \cdot \text{mol}^{-1}$, colourless plate, crystal size 0.02 x 0.18 x 0.22 mm³, monoclinic, space group $P2_1/c$, $a = 12.764(3) \text{ \AA}$, $b = 8.6044(6) \text{ \AA}$, $c = 7.2488(7) \text{ \AA}$, $\beta = 104.256(10)^\circ$, $V = 771.6(2) \text{ \AA}^3$, $T = 100 \text{ K}$, $Z = 4$, $D_{\text{calc}} = 1.765 \text{ g} \cdot \text{cm}^{-3}$, Mo- K_α radiation, $\lambda = 0.71073 \text{ \AA}$, $\mu = 5.262 \text{ mm}^{-1}$, Gaussian absorption correction ($T_{\text{min}} = 0.42296$, $T_{\text{max}} = 0.90081$), minimum and maximum estimated transmissions from the multi-scan scaling: 0.3985 and 0.9423 (SADABS), Bruker AXS Enraf-Nonius KappaCCD diffractometer, $2.88 < \theta < 33.21^\circ$, 24703 measured reflections, 2946 independent reflections ($R_{\text{int}} = 0.069$), 2454 reflections with $I > 2\sigma(I)$. Structure solved by direct methods and refined by full-matrix least-squares against F^2 to $R_1 = 0.0352$ [$I > 2\sigma(I)$], $wR_2 = 0.0941$, 91 parameters (G. M. Sheldrick, *Acta Cryst.* **2008**, A64, 112-122). $S = 1.153$, residual electron density +1.38 / -0.13 e \AA^{-3} . CCDC 880686.

Data were collected to a resolution of 0.65 \AA with an average redundancy of greater than 8 (see statistics, below). One reflection was lost, owing to the shadow cast by the beamstop. Although the face-indexed absorption correction was undertaken with as much care as possible, the observed negative residual electron density of -0.43 e\AA^{-3} , 0.82 \AA from O2, which is smaller than the negative residual electron density next to Br, may be due to the difficulty of accurately correcting for the effects of X-ray absorption for a plate composed of a substance with such a high linear absorption coefficient ($\mu = 5.262 \text{ mm}^{-1}$).

INTENSITY STATISTICS FOR DATASET

Resolution	#Data	#Theory	%Complete	Redundancy	Mean I	Mean I/s	R(int)	Rsigma
Inf - 1.80	158	162	97.5	13.04	121.7	38.04	0.0736	0.0236
1.80 - 1.42	158	158	100.0	11.45	77.3	36.48	0.0618	0.0224
1.42 - 1.24	161	162	99.4	11.15	49.8	35.55	0.0587	0.0221
1.24 - 1.12	171	171	100.0	10.67	47.6	35.78	0.0527	0.0222
1.12 - 1.03	175	175	100.0	10.33	28.1	28.79	0.0599	0.0246
1.03 - 0.97	166	166	100.0	10.01	26.2	27.66	0.0633	0.0259
0.97 - 0.92	164	164	100.0	9.68	23.9	28.91	0.0609	0.0260
0.92 - 0.88	165	165	100.0	8.76	19.4	24.96	0.0645	0.0309
0.88 - 0.84	202	202	100.0	8.50	13.8	19.88	0.0704	0.0366
0.84 - 0.81	157	157	100.0	8.18	14.8	19.78	0.0745	0.0372
0.81 - 0.78	207	207	100.0	7.42	11.1	16.20	0.0822	0.0448
0.78 - 0.75	241	241	100.0	6.70	9.2	13.78	0.0924	0.0553
0.75 - 0.73	175	175	100.0	6.50	8.4	12.72	0.1068	0.0616
0.73 - 0.71	198	198	100.0	5.95	7.0	11.14	0.1181	0.0741
0.71 - 0.69	235	235	100.0	5.49	6.0	9.31	0.1324	0.0879
0.69 - 0.67	233	234	99.6	4.74	5.0	7.21	0.1520	0.1132
0.67 - 0.65	151	158	95.6	3.72	3.5	4.88	0.1967	0.1684

0.75 - 0.65	1077	1085	99.3	5.41	6.1	9.36	0.1250	0.0876
Inf - 0.65	3117	3130	99.6	8.15	25.5	20.83	0.0683	0.0311

Merged [A], lowest resolution = 7.06 Angstroms, 636 outliers downweighted

The highest peak in the residual electron density map is 1.38 at 0.6381 0.3487 0.2177, 0.87 Å from Br1, and the deepest hole is -1.37 at 0.5612 0.4359 0.1603, 0.78 Å from Br1.

Table S4. Atomic coordinates and equivalent isotropic displacement parameters (\AA^2).
 U_{eq} is defined as one third of the trace of the orthogonalized U_{ij} tensor.

	x	y	z	U_{eq}
C(1)	0.7161(2)	0.2934(2)	0.2370(3)	0.016(1)
C(2)	0.7559(2)	0.1500(2)	0.2754(3)	0.013(1)
C(3)	0.8774(2)	0.1311(2)	0.3245(3)	0.018(1)
C(4)	0.9179(2)	0.0218(2)	0.1918(3)	0.017(1)
C(5)	0.8136(2)	-0.2126(2)	0.2096(3)	0.016(1)
C(6)	0.7104(2)	-0.1213(2)	0.1346(3)	0.017(1)
C(7)	0.6893(2)	0.0062(2)	0.2722(3)	0.016(1)
Br(1)	0.5677(1)	0.3461(1)	0.1767(1)	0.023(1)
O(1)	0.9099(1)	-0.1410(2)	0.2398(2)	0.018(1)
O(2)	0.8139(2)	-0.3506(2)	0.2461(3)	0.023(1)

Table S5. Selected bond lengths [Å] and angles [°].

C(1)-C(2)	1.338(3)	C(1)-Br(1)	1.891(2)		
C(2)-C(7)	1.499(3)	C(2)-C(3)	1.512(3)		
C(3)-C(4)	1.524(3)	C(4)-O(1)	1.453(2)		
C(5)-O(2)	1.217(2)	C(5)-O(1)	1.344(2)		
C(5)-C(6)	1.515(3)	C(6)-C(7)	1.550(3)		
C(2)-C(1)-Br(1)	125.20(16)	C(1)-C(2)-C(7)	125.02(18)	C(1)-C(2)-C(3)	117.57(17)
C(7)-C(2)-C(3)	117.41(15)	C(2)-C(3)-C(4)	113.92(16)	O(1)-C(4)-C(3)	112.89(16)
O(2)-C(5)-O(1)	117.29(19)	O(2)-C(5)-C(6)	122.65(19)	O(1)-C(5)-C(6)	120.05(16)
C(5)-C(6)-C(7)	114.16(17)	C(2)-C(7)-C(6)	113.99(16)	C(5)-O(1)-C(4)	121.21(16)

Table S6. Anisotropic displacement parameters (Å²).

The anisotropic displacement factor exponent takes the form:

$$-2\pi^2 [h^2 a^{*2} U_{11} + \dots + 2 h k a^* b^* U_{12}].$$

	U ₁₁	U ₂₂	U ₃₃	U ₂₃	U ₁₃	U ₁₂
C(1)	0.020(1)	0.012(1)	0.016(1)	0.000(1)	0.004(1)	0.002(1)
C(2)	0.015(1)	0.011(1)	0.014(1)	-0.001(1)	0.005(1)	0.000(1)
C(3)	0.016(1)	0.014(1)	0.022(1)	-0.004(1)	0.003(1)	-0.001(1)
C(4)	0.017(1)	0.012(1)	0.023(1)	0.001(1)	0.007(1)	-0.001(1)
C(5)	0.020(1)	0.010(1)	0.018(1)	-0.001(1)	0.006(1)	0.001(1)
C(6)	0.015(1)	0.013(1)	0.021(1)	-0.002(1)	0.004(1)	-0.001(1)
C(7)	0.017(1)	0.011(1)	0.023(1)	0.002(1)	0.009(1)	0.000(1)
Br(1)	0.024(1)	0.020(1)	0.024(1)	0.003(1)	0.006(1)	0.010(1)
O(1)	0.016(1)	0.013(1)	0.026(1)	0.001(1)	0.005(1)	0.002(1)
O(2)	0.029(1)	0.009(1)	0.033(1)	0.003(1)	0.010(1)	0.003(1)

References

1. Khan, A.; Medland, D. P.; Bhatia, G. S.; Eisai London Research Laboratories. Ltd. (UK), EP 1749829, 2007.
2. Polyak, I., Reetz, M. T. & Thiel, W. Quantum mechanical/molecular mechanical study on the mechanism of the enzymatic Baeyer-Villiger reaction. *J. Am. Chem. Soc.* **134**, 2732-2741, doi: 10.1021/Ja2103839 (2012).
3. Sherwood, P. *et al.* QUASI: A general purpose implementation of the QM/MM approach and its application to problems in catalysis. *J. Mol. Struct-Theochem.* **632**, 1-28, doi: 10.1016/S0166-1280(03)00285-9 (2003).
4. Billeter, S. R., Turner, A. J. & Thiel, W. Linear scaling geometry optimisation and transition state search in hybrid delocalised internal coordinates. *Phys. Chem. Chem. Phys.* **2**, 2177-2186 (2000).
5. Ahlrichs, R., Bar, M., Haser, M., Horn, H. & Kolmel, C. Electronic-structure calculations on workstation computers - the program system turbomole. *Chem. Phys. Lett.* **162**, 165-169 (1989).
6. Slater, J. C. A generalized self-consistent field method. *Phys. Rev.* **91**, 528-530 (1953).
7. Vosko, S. H., Wilk, L. & Nusair, M. Accurate spin-dependent electron liquid correlation energies for local spin-density calculations - a critical analysis. *Can. J. Phys.* **58**, 1200-1211 (1980).
8. Becke, A. D. Density-functional exchange-energy approximation with correct asymptotic-behavior. *Phys. Rev. A* **38**, 3098-3100 (1988).
9. Becke, A. D. Density-functional thermochemistry .3. The role of exact exchange. *J. Chem. Phys.* **98**, 5648-5652 (1993).
10. Stephens, P. J., Devlin, F. J., Chabalowski, C. F. & Frisch, M. J. Ab-initio calculation of vibrational absorption and circular-dichroism spectra using density-functional force-fields. *J. Phys. Chem-Us* **98**, 11623-11627 (1994).
11. Lee, C. T., Yang, W. T. & Parr, R. G. Development of the Colle-Salvetti correlation-energy formula into a functional of the electron-density. *Phys. Rev. B* **37**, 785-789 (1988).
12. Schafer, A., Huber, C. & Ahlrichs, R. Fully optimized contracted gaussian-basis sets of triple zeta valence quality for atoms Li to Kr. *J. Chem. Phys.* **100**, 5829-5835 (1994).
13. Smith, W. & Forester, T. R. DL_POLY_2.0: A general-purpose parallel molecular dynamics simulation package. *J. Mol. Graphics* **14**, 136-141 (1996).
14. MacKerell, A. D. *et al.* All-atom empirical potential for molecular modeling and dynamics studies of proteins. *J. Phys. Chem. B* **102**, 3586-3616 (1998).
15. Mirza, I. A. *et al.* Crystal structures of cyclohexanone monooxygenase reveal complex domain movements and a sliding cofactor. *J. Am. Chem. Soc.* **131**, 8848-8854, doi: 10.1021/Ja9010578 (2009).
16. Friesner, R. A. *et al.* Glide: A new approach for rapid, accurate docking and scoring. 1. Method and assessment of docking accuracy. *J. Med. Chem* **47**, 1739-1749, doi: 10.1021/Jm0306430 (2004).
17. Halgren, T. A. *et al.* Glide: A new approach for rapid, accurate docking and scoring. 2. Enrichment factors in database screening. *J. Med. Chem.* **47**, 1750-1759, doi: 10.1021/Jm030644s (2004).
18. Schrodinger, LLC; Portland, OR.
19. Bowers, K. J. *et al.* Proceedings of the ACM/IEEE Conference on Supercomputing (SC06), Tampa, Florida, 2006 November, 11-17.
20. Cerutti, D. S., Duke, R., Freddolino, P. L., Fan, H. & Lybrand, T. P. A vulnerability in popular molecular dynamics packages concerning Langevin and Andersen dynamics. *J. Chem. Theory Comput.* **4**, 1669-1680, doi: 10.1021/Ct8002173 (2008).
21. Arkin, I. T. *et al.* Mechanism of Na⁺/H⁺ antiporting. *Science* **317**, 799-803, doi: 10.1126/science.1142824 (2007).
22. Berendsen, H. J. C., Postma, J. P. M., Van Gunsteren, W.F., Hermans, J. *Intermolecular Forces*, ed. Pullmann B. (Reidel, Dordrecht, 1981), p331-.
23. Berweger, C. D., Vangunsteren, W. F. & Mullerplathe, F. Force-field parametrization by weak-coupling - reengineering Spc water. *Chem. Phys. Lett.* **232**, 429-436 (1995) .